Supporting Information

Synthesis and Structural Properties of para-Diselenopyrazines

Christopher Hüßler,[a] Martin C. Dietl,[a] Justin Kahle,[a] Eric F. Lopes,[a] Miku Kawamura,[a,b] Petra Krämer,[a] Frank Rominger,[a] Matthias Rudolph,[a] Iwao Hachiya,[b] and A. Stephen K. Hashmi*[a,c]

[a] Organisch-Chemisches Institut (OCI), Heidelberg University, Im Neuenheimer Feld 270, 69120 Heidelberg, Germany. E-mail: hashmi@hashmi.de

[b] Department of Applied Chemistry, Graduate School of Engineering, Mie University, Tsu Mie 514-8507, Japan. E-mail: hachiya@chem.mie-u.ac.jp

[c] Chemistry Department, Faculty of Science, King Abdulaziz University, Jeddah 21589, Saudi Arabia

Table of Contents

1 Experimental Procedures

1.1 General Information

Chemicals were bought from commercial suppliers (abcr, Acros, Alfa Aesar, BLDPharm, Carbolution, Chempur, Fluka, Merck, Sigma Aldrich and TCI) and used as delivered. Anhydrous solvents were dispensed from a solvent purification system MB SPS-800. Solvents were degassed by freeze-pump-thaw technique. Deuterated solvents were bought from Eurisotop and Sigma Aldrich.

Melting points (mp) were measured in open glass capillaries on a Stuart SMP10 melting point apparatus and are uncorrected.

R_f-values were determined by analytical thin layer chromatography (TLC) on aluminium sheets coated with silica gel produced by Macherey-Nagel (ALUGRAM® Xtra SIL G/25 UV_{254}). Detections was accomplished using UV-light (254 and 365 nm) or a TLC staining solution (vanillin and ninhydrine).

Nuclear magnetic resonance (NMR) spectra were, if not mentioned otherwise, recorded at room temperature at the organic chemistry department of Heidelberg University under the supervision of Dr. J. Graf on the following spectrometers: Bruker Avance III 300 (300 MHz), Bruker Avance DRX 300 (300 MHz), Bruker Fourier 300 (300 MHz), Bruker Avance III 400 (400 MHz), Bruker Avance III 500 (500 MHz), Bruker Avance III 600 (600 MHz), Bruker Avance NEO 700 (700 MHz). Chemical shifts δ are given in ppm and coupling constants *J* in Hz. Spectra were referenced to residual solvent protons according to Fulmer *et al.*[1] or for TCE-d_2 to 6.00 ppm (^{1}H) and 73.8 ppm (^{13}C) respectively. The following abbreviations were used to describe the observed multiplicities: for ^{1}H NMR spectra: s = singlet, d = doublet, t = triplet, q = quartet, qui = quintet, sext = sextet, sept = septet, m = multiplet, dd = doublet of doublets, td = triplet of doublets, dt = doublet of triplets, br = broad signal; for ^{13}C{^{1}H} NMR spectra: s = quarternary carbon, d = CH carbon, t = CH_2 carbon and q = CH_3 carbon. ^{13}C{^{1}H} NMR spectra are proton decoupled and interpreted with help of DEPT- and 2D spectra. All spectra were integrated and processed using MestreNova software.

High-resolution mass spectra (HR-MS) were recorded at the chemistry department of Heidelberg University under the supervision of Dr. J. Gross on the following spectrometers: JEOL AccuTOF GCx (EI), Bruker ApexQe hybrid 9.4 T FT-ICR (ESI, MALDI, DART), Finnigan LCQ (ESI), Bruker AutoFlex Speed (MALDI) and Bruker timsTOFfleX (ESI, MALDI).

Infrared spectra were recorded from a neat powder or oil on a FT-IR spectrometer (Bruker LUMOS) with a Germanium ATR-crystal. For the most significant bands the wave numbers are given.

UV-Vis spectra were recorded on a Jasco UV-Vis V-660. Fluorescence spectra were recorded on a Jasco FP6500. Quantum yields (QY) were recorded on a PTI QuantaMaster 40 with Ulbricht Sphere.

Cyclic voltammograms were measured on a VERSASTAT3-200 potentiostat, using a glassy carbon working electrode, a silver reference electrode and a platinum/titanium counter electrode. Measurements were carried out in a 0.1 M tetrabutylammonium hexafluorophosphate solution in anhydrous and degassed DCM. Ferrocene/ferrocenium was used as internal standard.

X-ray crystallography was carried out at the chemistry department of Heidelberg University under the supervision of Dr. F. Rominger on the following instruments: Bruker Smart APEX II Quazar (with Mo-microsource) and Stoe Stradivari (with Co-microsource and Pilatus detector). The structures were processed with Mercury 4.3.0.

For flash column chromatography silica gel (Sigma-Aldrich, pore size 60 Å, 70-230 mesh, 63-200 μm) or aluminium oxide (Honeywell, pore size 60 Å, activated, neutral) was used as stationary phase. As

eluents different mixtures of petroleum ether (PE), ethyl acetate (EA) or dichloromethane (DCM) were used.

1.2 General Procedures

General Procedure 1 (GP1): Sonogashira cross coupling

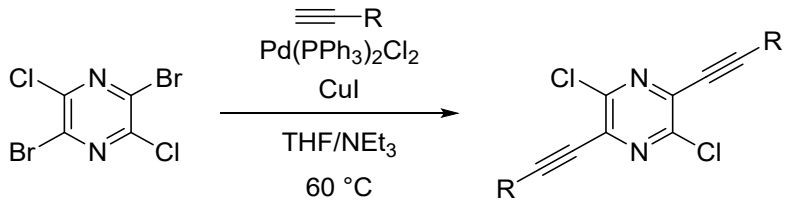

In a heat gun-dried Schlenk flask under an atmosphere of nitrogen, 2,5-dibromo-3,6-dichloropyrazine (1.00 eq.), $Pd(PPh_3)_2Cl_2$ (3 mol %) and CuI (3 mol %) were dissolved in a degassed mixture of THF (20 ml) and triethylamine (20 ml). After stirring for 5 min, the corresponding alkyne (2.05 eq.) was added. The mixture was stirred at 60 °C overnight. The reaction was cooled and solvents were removed under reduced pressure. The crude product was purified by flash column chromatography.

General Procedure 2 (GP2): Nucleophilic cyclization to Diselenopyrazines

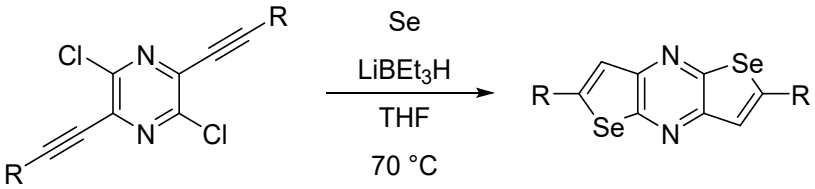

In a heat gun-dried Schlenk flask under an atmosphere of nitrogen, Selenium (2.30 eq.) was suspended in dry THF (20 ml). $LiBEt_3H$ (2.50 eq.) was added and the mixture was stirred for 30 min. Bis-ethynylpyrazine (1.00 eq.) was added and the mixture was stirred at 70 °C overnight. The crude product was purified by precipitation or column chromatography.

1.3 Synthesis of Compounds

2,5-dibromo-3,6-dichloropyrazine (1)

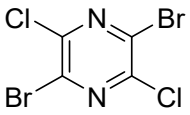

To a solution of 5-bromo-6-chloropyrazin-2-amine (10.0 g, 48.0 mmol, 1.00 eq.) in MeOH (100 ml) was added N-chlorosuccinimide (7.05 g, 52.8 mmol, 1.10 eq.) and the resulting mixture was stirred at 50 °C overnight. Water (500 ml) was added and the colorless precipitate was collected by filtration and dried under reduced pressure. The compound was dissolved in HBr (48 wt%, 320 ml) and THF (160 ml). The mixture was cooled to 0 °C and $NaNO_2$ (8.21 g, 119 mmol, 2.50 eq.) was added in small portions. The reaction mixture was stirred at rt for 1 h. Afterwards, KOH was added until neutralization of the mixture and the crude product was extracted with EA, dried over Na_2SO_4 and the solvent was removed under reduced pressure. Purification by column chromatography (silica gel, PE/EA 30:1) yielded a colorless solid (8.10 g, 26.4 mmol, 56 %).

$^{13}C\{^1H\}$ NMR (75 MHz, $CDCl_3$): δ = 146.8 (s), 136.5 (s) ppm.

The spectroscopic data correspond to those previously reported in the literature.[2]

2,5-Dichloro-3,6-bis(triisopropylsilyl)pyrazine (2a)

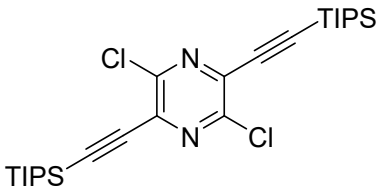

The reaction was carried out according to **GP1** with **1** (500 mg, 1.63 mmol, 1.00 eq.), $Pd(PPh_3)_2Cl_2$ (34.3 mg, 48.9 µmol, 0.03 eq.), CuI (9.31 mg, 48.9 µmol, 0.03 eq.) and triisopropylsilylacetylene (609 mg, 3.34 mmol, 2.05 eq.). Purification by column chromatography (silica gel, PE) yielded a colorless solid (617 mg, 1.21 mmol, 75 %).

^1H NMR (300 MHz, $CDCl_3$): δ = 1.23 – 1.12 (m, 42H) ppm.

The spectroscopic data correspond to those previously reported in the literature.[3]

2,5-Dichloro-3,6-bis(methylethynyl)pyrazine (2c)

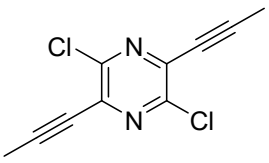

The reaction was carried out according to **GP1** with **1** (700 mg, 2.28 mmol, 1.00 eq.), $Pd(PPh_3)_2Cl_2$ (48.1 mg, 68.5 µmol, 0.03 eq.), CuI (13.0 mg, 68.5 µmol, 0.03 eq.) and propyne (187 mg, 4.68 mmol, 2.05 eq.). Purification by column chromatography (silica gel, PE/DCM 20:1) yielded a light brown solid (314 mg, 1.40 mmol, 61 %).

Mp: 156-159 °C; $\mathbf{R_f}$: 0.43 (silica gel, PE/EA 10:1); **^1H NMR** (400 MHz, $CDCl_3$): δ = 2.20 (s, 6H) ppm; **$^{13}C\{^1H\}$ NMR** (100 MHz, $CDCl_3$): δ = 147.3 (s), 136.1 (s), 98.7 (s), 75.5 (s), 5.1 (q) ppm; **HR-MS** (EI+): *m/z* calculated for $[C_{10}H_6N_2Cl_2]^+$, $[M]^+$: 223.99026, found: 223.99001; **IR** (ATR): ν [cm^{-1}] = 2967, 2916,

2732, 2466, 2316, 2235, 1419, 1294, 1247, 1183, 1141, 1032, 997, 739, 686, 641; **UV-VIS** (DCM): λ_{max} [nm] = 275, 340; **Fluorescence** (DCM): λ_{ex} [nm] = 340, λ_{max} [nm] = 375; **Quantum yield** (DCM): Φ = 7 %.

2,5-Dichloro-3,6-bis(butylethynyl)pyrazine (2d)

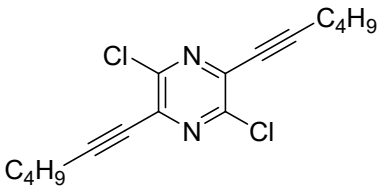

The reaction was carried out according to **GP1** with **1** (500 mg, 1.63 mmol, 1.00 eq.), $Pd(PPh_3)_2Cl_2$ (34.3 mg, 48.9 µmol, 0.03 eq.), CuI (9.31 mg, 48.9 µmol, 0.03 eq.) and hexyne (275 mg, 3.34 mmol, 2.05 eq.). Purification by column chromatography (silica gel, PE/DCM 10:1 → 5:1 → 2:1) yielded an orange solid (430 mg, 1.39 mmol, 85 %).

^{1}H NMR (700 MHz, $CDCl_3$): δ = 2.54 (t, *J* = 7.1 Hz, 4H), 1.65 (qui, *J* = 7.3 Hz, 4H), 1.51 (sext, *J* = 7.4 Hz, 4H), 0.95 (t, *J* = 7.4 Hz, 6H) ppm.

The spectroscopic data correspond to those previously reported in the literature.[4]

2,5-Dichloro-3,6-bis(phenylethynyl)pyrazine (2e)

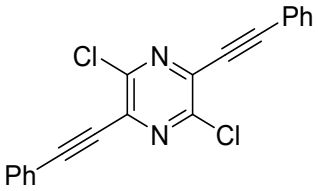

The reaction was carried out according to **GP1** with **1** (3.00 g, 9.78 mmol, 1.00 eq.), $Pd(PPh_3)_2Cl_2$ (206 mg, 294 µmol, 0.03 eq.), CuI (55.9 mg, 294 µmol, 0.03 eq.) and phenylacetylene (2.10 g, 20.5 mmol, 2.05 eq.). Purification by column chromatography (silica gel, PE/DCM 5:1 → DCM) yielded a pale yellow solid (3.40 g, 9.74 mmol, 99 %).

^{1}H NMR (300 MHz, $CDCl_3$): δ = 7.70 – 7.63 (m, 4H), 7.52 – 7.36 (m, 6H) ppm.

The spectroscopic data correspond to those previously reported in the literature.[3]

2,5-Dichloro-3,6-bis(4-n-pentylphenylethynyl)pyrazine (2f)

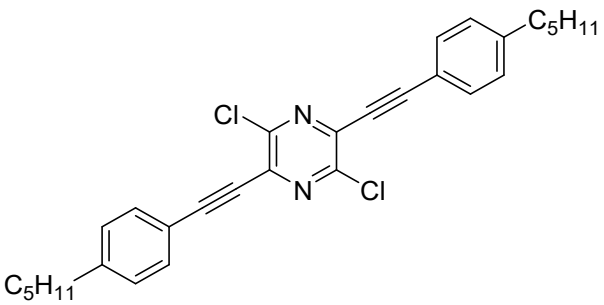

The reaction was carried out according to **GP1** with **1** (500 mg, 1.63 mmol, 1.00 eq.), $Pd(PPh_3)_2Cl_2$ (34.3 mg, 48.9 µmol, 0.03 eq.), CuI (9.31 mg, 48.9 µmol, 0.03 eq.) and 4-n-pentylphenylacetylene (576 mg, 3.34 mmol, 2.05 eq). Purification by column chromatography (silica gel, PE/DCM 10:1) yielded a yellow solid (585 mg, 1.20 mmol, 73 %).

^{1}H NMR (600 MHz, $CDCl_3$): δ = 7.56 (d, J = 8.1 Hz, 4H), 7.22 (d, J = 8.2 Hz, 4H), 2.64 (t, J = 7.8 Hz, 4H), 1.63 (qui, J = 7.5 Hz, 4H), 1.38 – 1.28 (m, 8H), 0.90 (t, J = 7.0 Hz, 6H) ppm.

The spectroscopic data correspond to those previously reported in the literature.[4]

2,5-Dichloro-3,6-bis(3,5-bis(trifluoromethyl)phenylethynyl)pyrazine (2g)

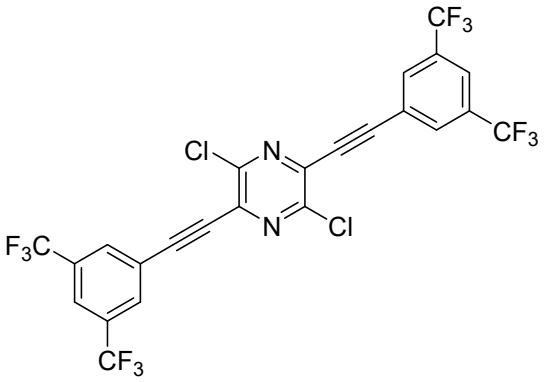

The reaction was carried out according to **GP1** with **1** (250 mg, 815 µmol, 1.00 eq.), $Pd(PPh_3)_2Cl_2$ (17.2 mg, 24.5 µmol, 0.03 eq.), CuI (4.67 mg, 24.5 µmol, 0.03 eq.) and 3,5-bis(trifluoromethyl)phenylacetylene (398 mg, 1.67 mmol, 2.05 eq.). Purification by column chromatography (silica gel, PE/DCM 5:1) yielded a yellow solid (453 mg, 729 µmol, 89 %).

^{1}H NMR (600 MHz, $CDCl_3$): δ = 8.09 (s, 4H), 7.96 (s, 2H) ppm.

The spectroscopic data correspond to those previously reported in the literature.[4]

2,2'-Bis(triisopropylsilyl)diseleno[2,3-b:2',3'-e]pyrazine (3a)

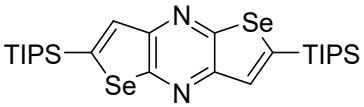

The reaction was carried out according to **GP2** with **2a** (1.00 g, 1.96 mmol, 1.00 eq.), Se (356 mg, 4.51 mmol, 2.30 eq.) and $LiBEt_3H$ (520 mg, 4.90 mmol, 2.50 eq., 1M in THF). The crude product was filtered over Celite® and precipitated with pentane to yield a light brown solid (400 mg, 668 µmol, 34 %).

Mp: 215-217 °C; **R_f**: 0.76 (silica gel, PE/EA 10:1); **^{1}H NMR** (400 MHz, $CDCl_3$): δ = 7.97 (s, 2H), 1.43(sept, J = 7.3 Hz, 6H), 1.19 (s, 18H), 1.17 (s, 18H) ppm; **^{13}C{^{1}H} NMR** (100 MHz, $CDCl_3$): δ = 159.5 (s), 150.4 (s), 149.8 (s), 133.8 (d), 18.7 (q), 12.1 (d) ppm; **^{77}Se{^{1}H} NMR** (76 MHz, $CDCl_3$): δ = 563.1 (s) ppm; **HR-MS** (EI+): *m/z* calculated for $[C_{26}H_{44}N_2Si_2Se_2]^+$, $[M]^+$: 600.13680, found: 600.14056; **IR** (ATR): ν [cm^{-1}] = 3053, 2939, 2886, 2862, 2832, 1735, 1508, 1461, 1411, 1366, 1291, 1230, 1176, 1118, 1072, 1015, 995, 904, 883, 827, 680, 649; **UV-VIS** (DCM): λ_{max} [nm] = 283, 352.

Diseleno[2,3-b:2',3'-e]pyrazine (3b)

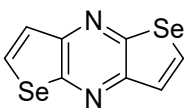

In a heatgun-dried Schlenk-flask under an atmosphere of nitrogen, **3a** (106 mg, 177 µmol, 1.00 eq.) was dissolved in dry toluene. Tetrabutylammonium fluoride (278 mg, 1.06 mmol, 6.00 eq., 1M in

THF) was added and the mixture was stirred at 100 °C overnight. Purification by column chromatography (silica gel, PE/EA 5:1) yielded a yellow solid (46.0 mg, 161 μmol, 91 %).

Mp: 232-233 °C; $\mathbf{R_f}$: 0.27 (silica gel, PE/EA 10:1); **^{1}H NMR** (400 MHz, $CDCl_3$): δ = 8.41 (d, J = 6.6 Hz, 2H), 7.74 (d, J = 6.5 Hz, 2H) ppm; **^{13}C{^{1}H} NMR** (100 MHz, $CDCl_3$): δ = 157.0 (s), 149.2 (s), 135.1 (d), 125.5 (d) ppm; **^{77}Se{^{1}H} NMR** (76 MHz, $CDCl_3$): δ = 500.0 (s) ppm; **HR-MS** (EI+): *m/z* calculated for $[C_8H_4N_2Se_2]^+$, $[M]^+$: 287.86994, found: 287.86898; **IR** (ATR): ν [cm^{-1}] = 3082, 3062, 2125, 1797, 1660, 1603, 1543, 1510, 1467, 1425, 1293, 1250, 1217, 1114, 1052, 901, 817, 757, 726, 643; **UV-VIS** (DCM): λ_{max} [nm] = 271, 336.

2,2'-Dimethyldiseleno[2,3-b:2',3'-e]pyrazine (3c)

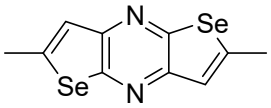

The reaction was carried out according to **GP2** with **2c** (90 mg, 400 μmol, 1.00 eq.), Se (73 mg, 920 μmol, 2.30 eq.) and $LiBEt_3H$ (106 mg, 1.00 mmol, 2.50 eq., 1M in THF). The crude product was filtered over Celite® and precipitated with pentane to yield a beige solid (29 mg, 92.3 μmol, 23 %).

Mp: 259-263 °C; $\mathbf{R_f}$: 0.18 (silica gel, PE/EA 10:1); **^{1}H NMR** (400 MHz, $CDCl_3$): δ = 7.28 (q, J = 1.4 Hz, 2H), 2.76 (d, J = 1.4 Hz, 6H) ppm; **^{13}C{^{1}H} NMR** (100 MHz, $CDCl_3$): δ = 157.2 (s), 150.5 (s), 149.7 (s), 122.8 (d), 20.4 (q) ppm; **^{77}Se{^{1}H} NMR** (76 MHz, $CDCl_3$): δ = 519.4 (s) ppm; **HR-MS** (EI+): *m/z* calculated for $[C_{10}H_8N_2Se_2]^+$, $[M]^+$: 315.90124, found: 315.89727; **IR** (ATR): ν [cm^{-1}] = 3126, 3032, 2963, 2910, 2840, 2727, 2228, 1710, 1566, 1454, 1426, 1377, 1298, 1253, 1205, 1118, 1098, 1033, 857, 839, 737, 660, 638; **UV-VIS** (DCM): λ_{max} [nm] = 271, 343.

2,2'-Dibuyldiseleno[2,3-b:2',3'-e]pyrazine (3d)

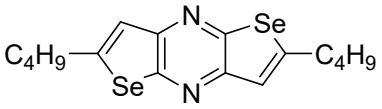

The reaction was carried out according to **GP2** with **2d** (200 mg, 647 μmol, 1.00 eq.), Se (105 mg, 1.33 mmol, 2.30 eq.) and $LiBEt_3H$ (158 mg, 1.49 mmol, 2.50 eq., 1M in THF). The crude product was filtered over Celite® to yield a dark brown amorphous solid (79 mg, 198 μmol, 31 %).

$\mathbf{R_f}$: 0.33 (silica gel, PE/EA 10:1); **^{1}H NMR** (400 MHz, $CDCl_3$): δ = 7.30 (t, J = 1.2 Hz, 2H), 3.03 (td, J = 7.5, 1.3 Hz, 4H), 1.77 (qui, J = 7.5 Hz, 4H), 1.48 (sxt, J = 7.4 Hz, 4H), 0.98 (t, J = 7.4 Hz, 6H) ppm; **^{13}C{^{1}H} NMR** (100 MHz, $CDCl_3$): δ = 156.9 (s), 149.5 (s), 121.6 (d), 34.3 (t), 33.6 (t), 22.3 (t), 13.9 (q) ppm; **^{77}Se{^{1}H} NMR** (76 MHz, $CDCl_3$): δ = 504.4 (s) ppm; **HR-MS** (EI+): *m/z* calculated for $[C_{16}H_{20}N_2Se_2]^+$, $[M]^+$: 399.99514, found: 399.99671; **IR** (ATR): ν [cm^{-1}] = 2954, 2927, 2865, 2228, 1561, 1501, 1453, 1394, 1378, 1296, 1262, 1219, 1185, 1117, 1059, 818, 726, 624; **UV-VIS** (DCM): λ_{max} [nm] = 273, 347.

2,2'-Diphenyldiseleno[2,3-b:2',3'-e]pyrazine (3e)

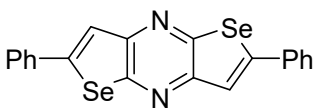

The reaction was carried out according to **GP2** with **2e** (100 mg, 286 μmol, 1.00 eq.), Se (52.0 mg, 659 μmol, 2.30 eq.) and $LiBEt_3H$ (75.8 mg, 716 μmol, 2.50 eq., 1M in THF). The crude product was filtered over Celite® and precipitated with pentane to yield a dark brown solid (41.0 mg, 93.6 mmol, 33 %).

Mp: 159-163 °C; **R_f**: 0.13 (silica gel, PE/EA 10:1); **^{1}H NMR** (400 MHz, $CDCl_3$): δ = 7.86 (s, 2H), 7.73-7.71 (m, 4H), 7.50-7.43 (m, 6H) ppm; **^{13}C{^{1}H} NMR** (100 MHz, $CDCl_3$): δ = 157.5 (s), 152.7 (s), 150.6 (s), 135.6 (s), 129.9 (d), 129.4 (d), 127.0 (d), 120.3 (d) ppm; **^{77}Se{^{1}H} NMR** (76 MHz, $CDCl_3$): δ = 491.6 (s) ppm; **HR-MS** (EI+): *m/z* calculated for $[C_{20}H_{12}N_2Se_2]^+$, $[M]^+$: 439.93254, found: 439.92785; **IR** (ATR): ν [cm^{-1}] = 3057, 2216, 1939, 1865, 1804, 1730, 1674, 1596, 1543, 1488, 1451, 1332, 1297, 1253, 1223, 1182, 1117, 1072, 1027, 904, 841, 832, 752, 682, 648; **UV-VIS** (DCM): λ_{max} [nm] = 281, 299, 382.

2,2'-Bis(4-pentylphenyl)diseleno[2,3-b:2',3'-e]pyrazine (3f)

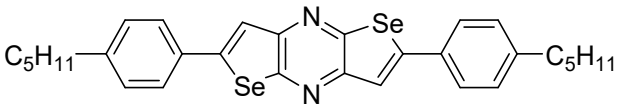

The reaction was carried out according to **GP2** with **2f** (200 mg, 409 µmol, 1.00 eq.), Se (66.1 mg, 838 µmol, 2.30 eq.) and $LiBEt_3H$ (100 mg, 940 µmol, 2.50 eq., 1M in THF). The crude product was filtered over Celite® and precipitated with pentane to yield a dark yellow solid (70.0 mg, 121 µmol, 30 %).

Mp: 209-210 °C; **R_f**: 0.47 (silica gel, PE/EA 10:1); **^{1}H NMR** (400 MHz, $CDCl_3$): δ = 7.80 (s, 2H), 7.62 (d, J = 8.2 Hz, 4H), 7.28 (d, J = 8.3 Hz, 4H), 2.67 (t, J = 7.9 Hz, 4H), 1.70-1.62 (m, 4H), 1.37-1.33 (m, 8H), 0.91 (t, J = 6.9 Hz, 6H) ppm; **^{13}C{^{1}H} NMR** (100 MHz, $CDCl_3$): δ = 157.3 (s), 152.7 (s), 150.6 (s), 145.2 (s), 133.1 (s), 129.4 (d), 126.9 (d), 119.6 (d), 35.9 (t), 31.6 (t), 31.1 (t), 22.7 (t), 14.2 (q) ppm; **^{77}Se{^{1}H} NMR** (76 MHz, $CDCl_3$): δ = 489.2 (s) ppm; **HR-MS** (EI+): *m/z* calculated for $[C_{30}H_{32}N_2Se_2]^+$, $[M]^+$: 580.08904, found: 580.08751; **IR** (ATR): ν [cm^{-1}] = 3019, 2957, 2930, 2855, 1923, 1898, 1869, 1739, 1606, 1546, 1504, 1468, 1452, 1408, 1307, 1289, 1254, 1227, 1180, 1115, 1015, 913, 821, 800, 723, 657, 647, 616; **UV-VIS** (DCM): λ_{max} [nm] = 281, 310, 396.

2,2'-Bis(3,5-bis(trifluoromethyl)phenyl)diseleno[2,3-b:2',3'-e]pyrazine (3g)

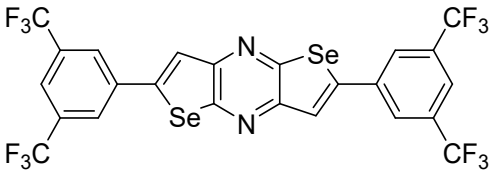

The reaction was carried out according to **GP2** with **2g** (100 mg, 161 µmol, 1.00 eq.), Se (29.2 mg, 370 µmol, 2.30 eq.) and $LiBEt_3H$ (42.6 mg, 402 µmol, 2.50 eq., 1M in THF). The crude product was filtered over Celite® and precipitated with pentane to yield a brown solid (41.0 mg, 57.7 µmol, 36 %).

Mp: >300 °C; **R_f**: 0.41 (silica gel, PE/EA 10:1); **^{1}H NMR** (400 MHz, $CDCl_3$): δ = 8.11 (s, 4H), 8.01 (s, 2H), 7.95 (s, 2H) ppm; **^{13}C{^{1}H} NMR** (100 MHz, $CDCl_3$): δ = 158.1 (s), 150.5 (s), 149.4 (s), 137.7 (s), 133.2 (s), 127.0 (d), 124.2 (s), 123.0 (d), 122.0 (s) ppm; **^{19}F{^{1}H} NMR** (283 MHz, $CDCl_3$): δ = 62.9 (s) ppm; **^{77}Se{^{1}H} NMR** (76 MHz, $CDCl_3$): δ = 503.7 (s) ppm; **HR-MS** (ESI+): *m/z* calculated for $[C_{24}H_9F_{12}N_2Se_2]^+$, $[M+H]^+$: 712.89080, found: 712.88990; **IR** (ATR): ν [cm^{-1}] = 3104, 3036, 1619, 1469, 1433, 1370, 1278, 1255, 1168, 1126, 983, 909, 894, 844, 753, 696, 680, 638; **UV-VIS** (DCM): λ_{max} [nm] = 284, 381.

2 NMR Spectra

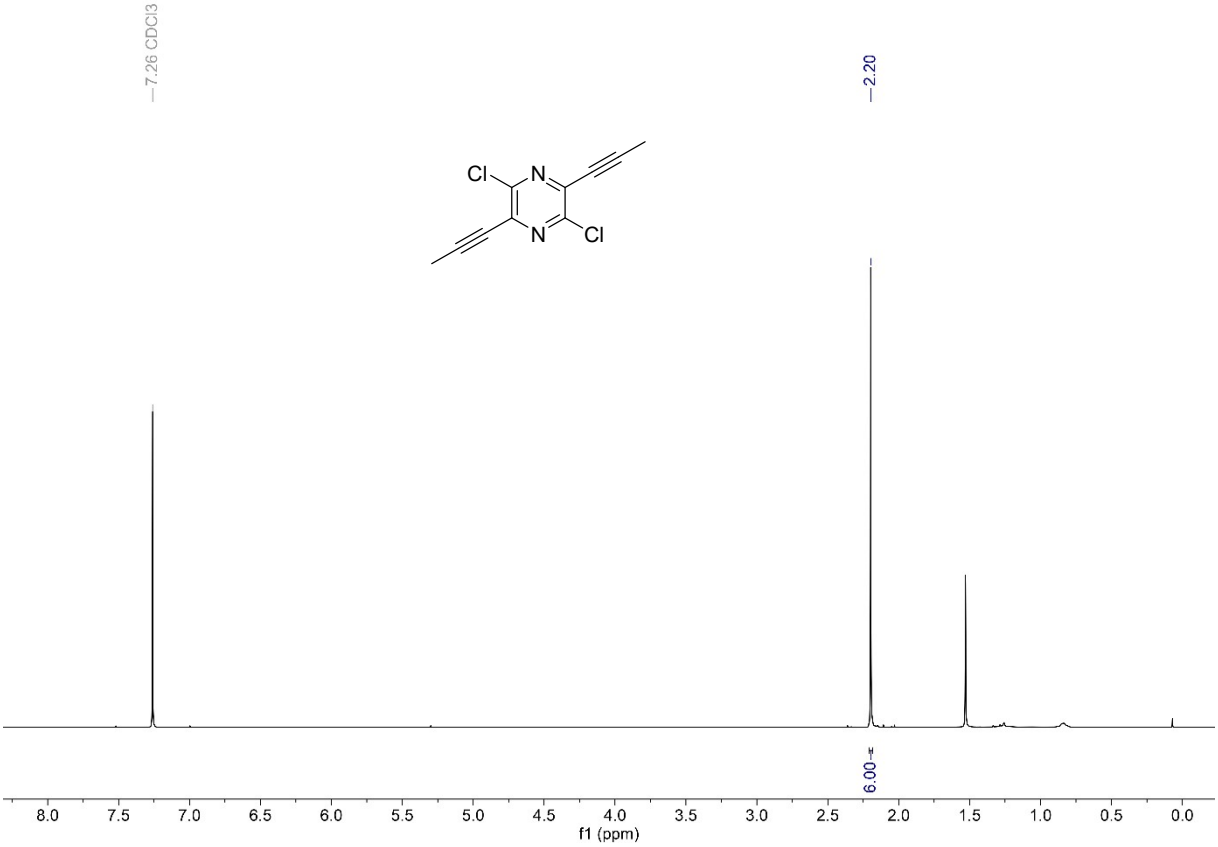

Figure S1. ^{1}H NMR spectrum (400 MHz, $CDCl_3$) of **2c**.

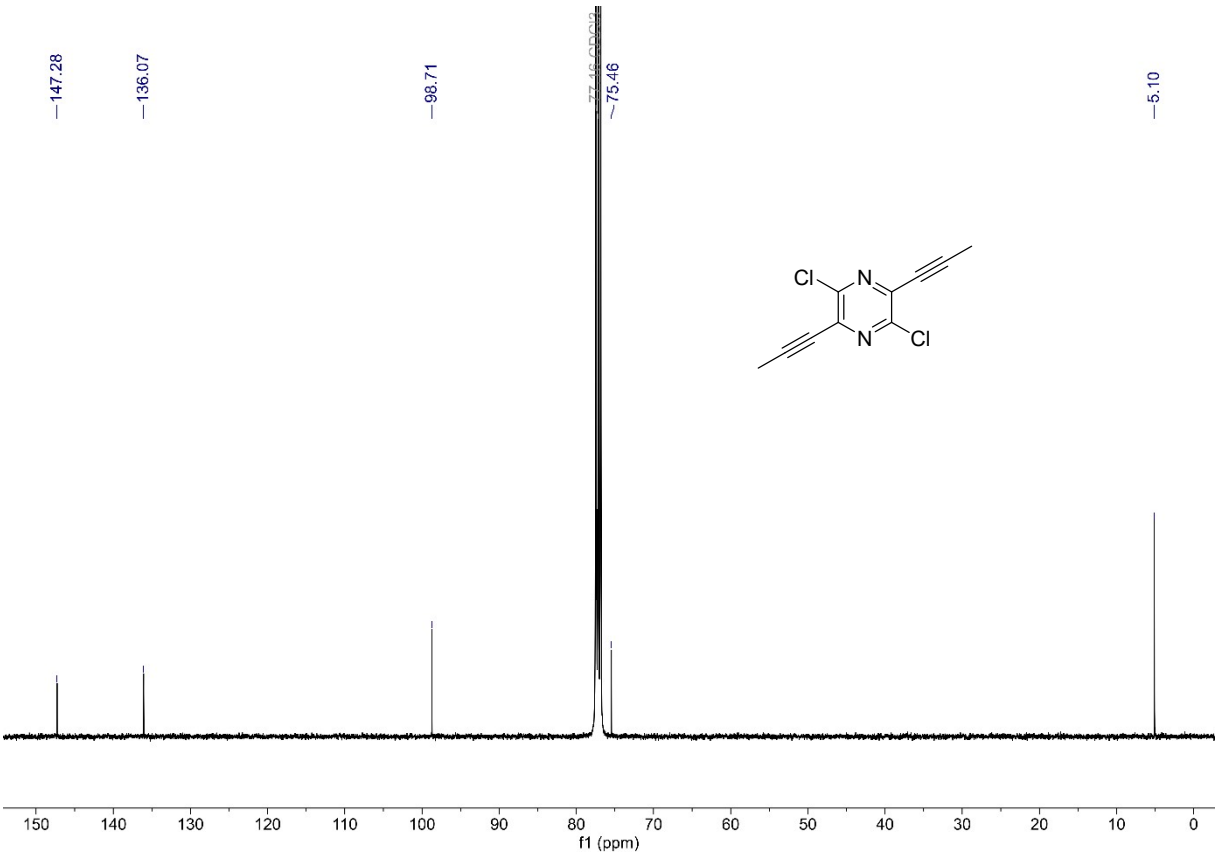

Figure S2. $^{13}C\{^{1}H\}$ NMR spectrum (101 MHz, $CDCl_3$) of **2c**.

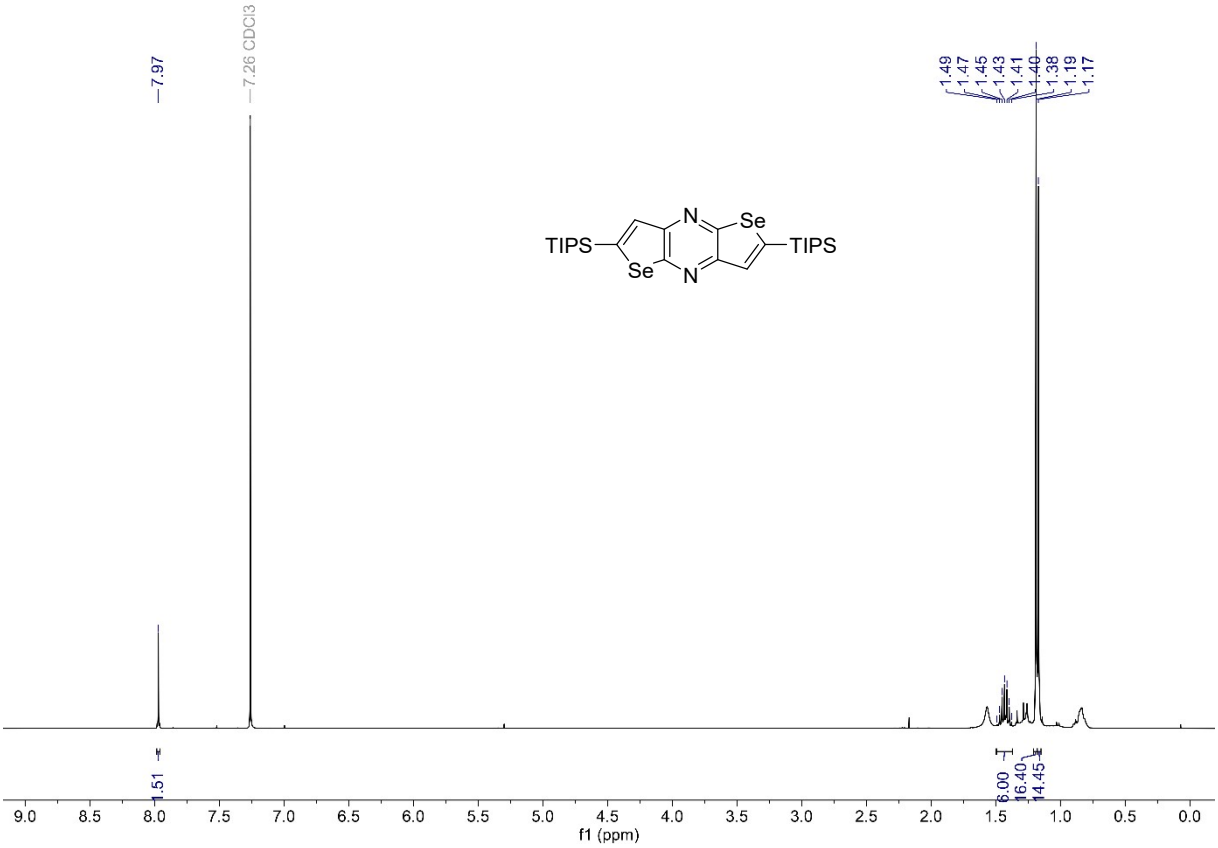

Figure S3. ^{1}H NMR spectrum (400 MHz, $CDCl_3$) of **3a**.

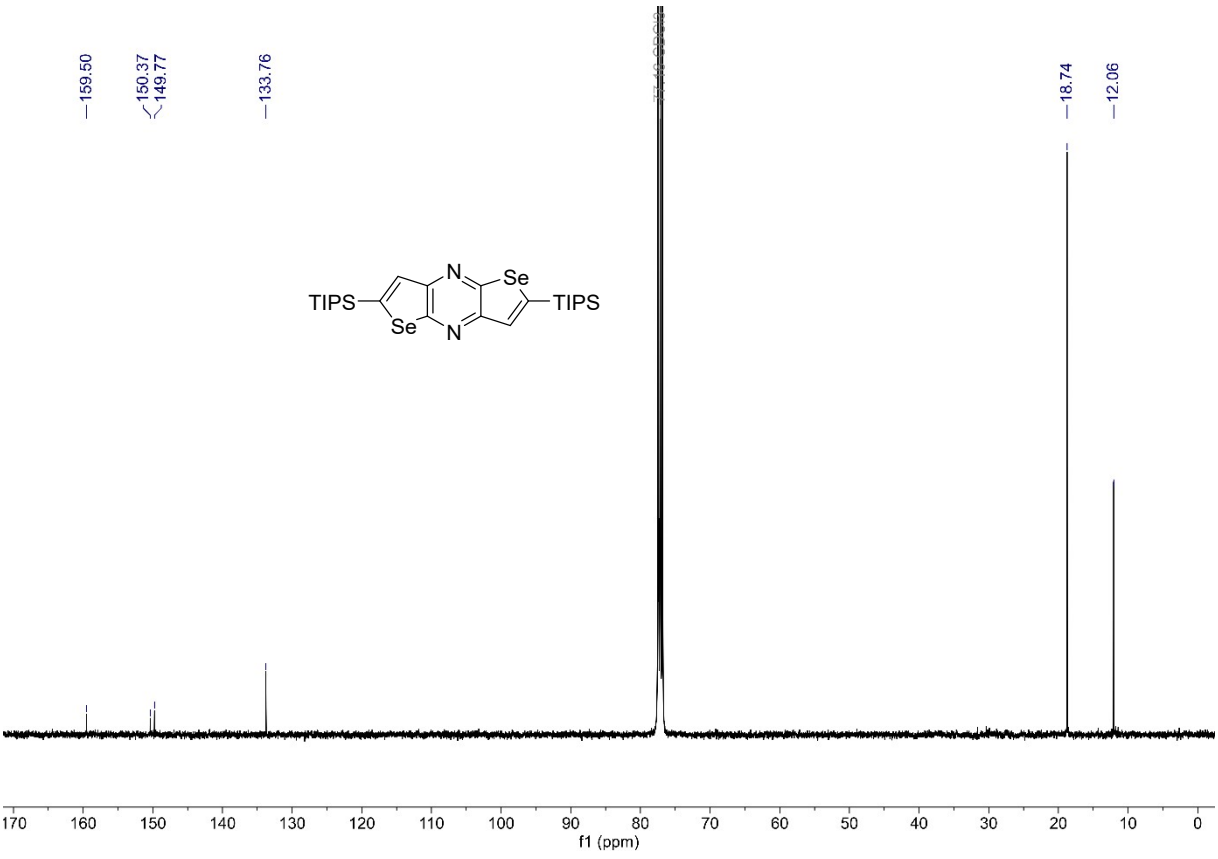

Figure S4. $^{13}C\{^{1}H\}$ NMR spectrum (101 MHz, $CDCl_3$) of **3a**.

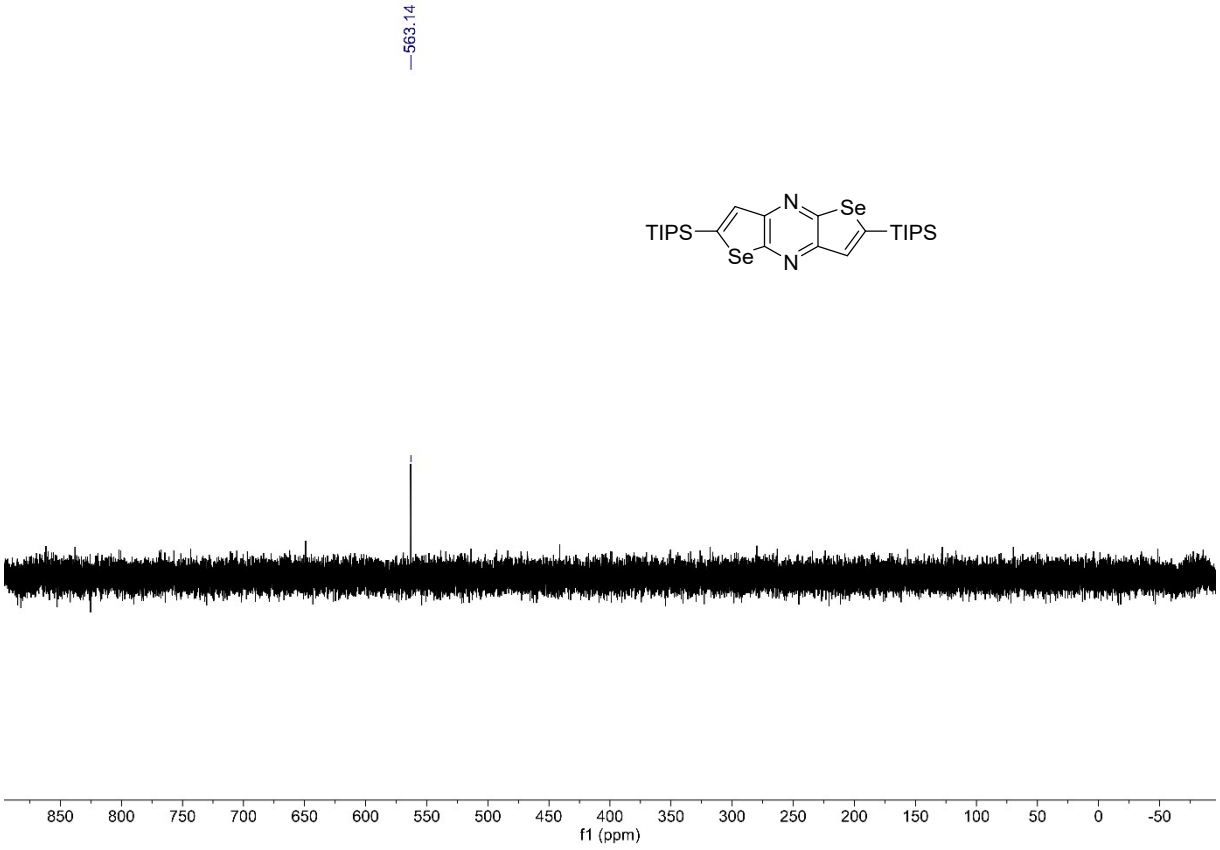

Figure S5. $^{77}Se\{^{1}H\}$ NMR spectrum (76 MHz, $CDCl_3$) of **3a**.

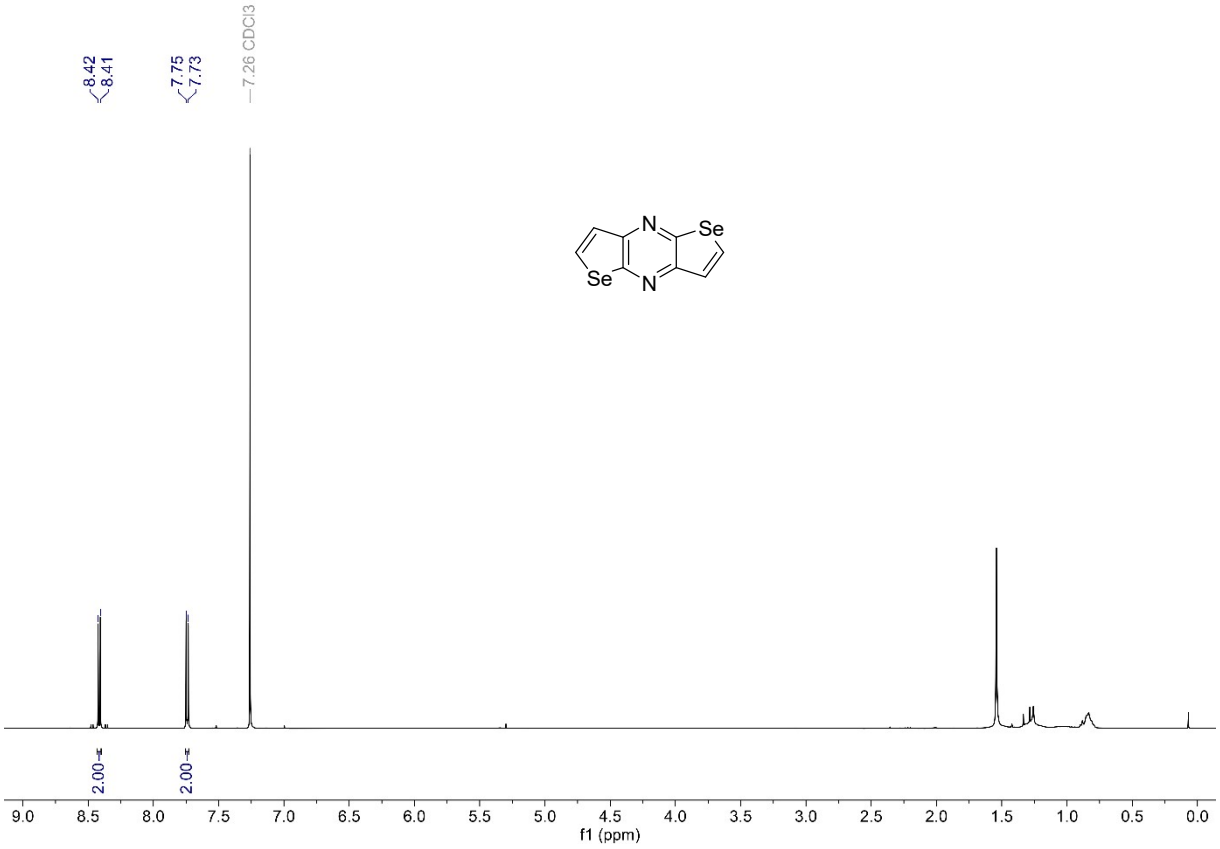

Figure S6. ^{1}H NMR spectrum (400 MHz, $CDCl_3$) of **3b**.

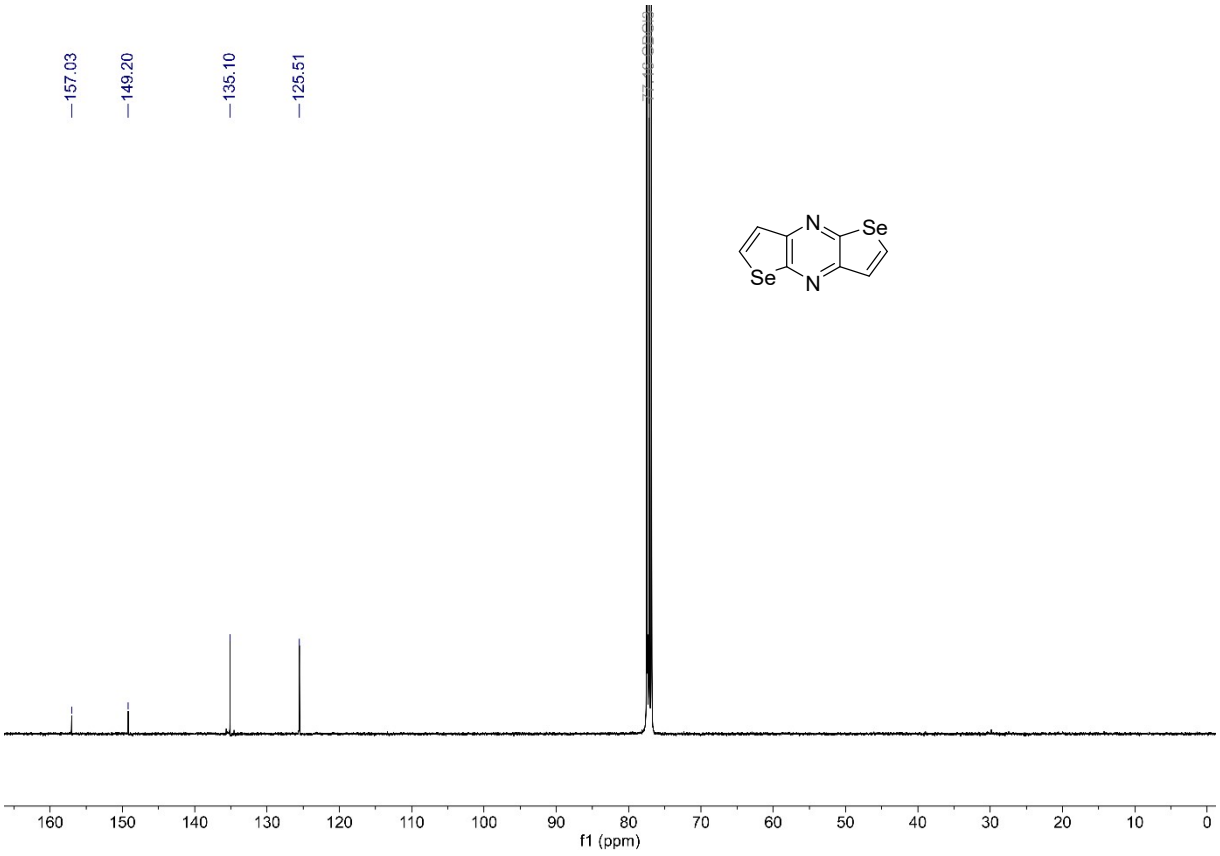

Figure S7. $^{13}C\{^{1}H\}$ NMR spectrum (101 MHz, $CDCl_3$) of **3b**.

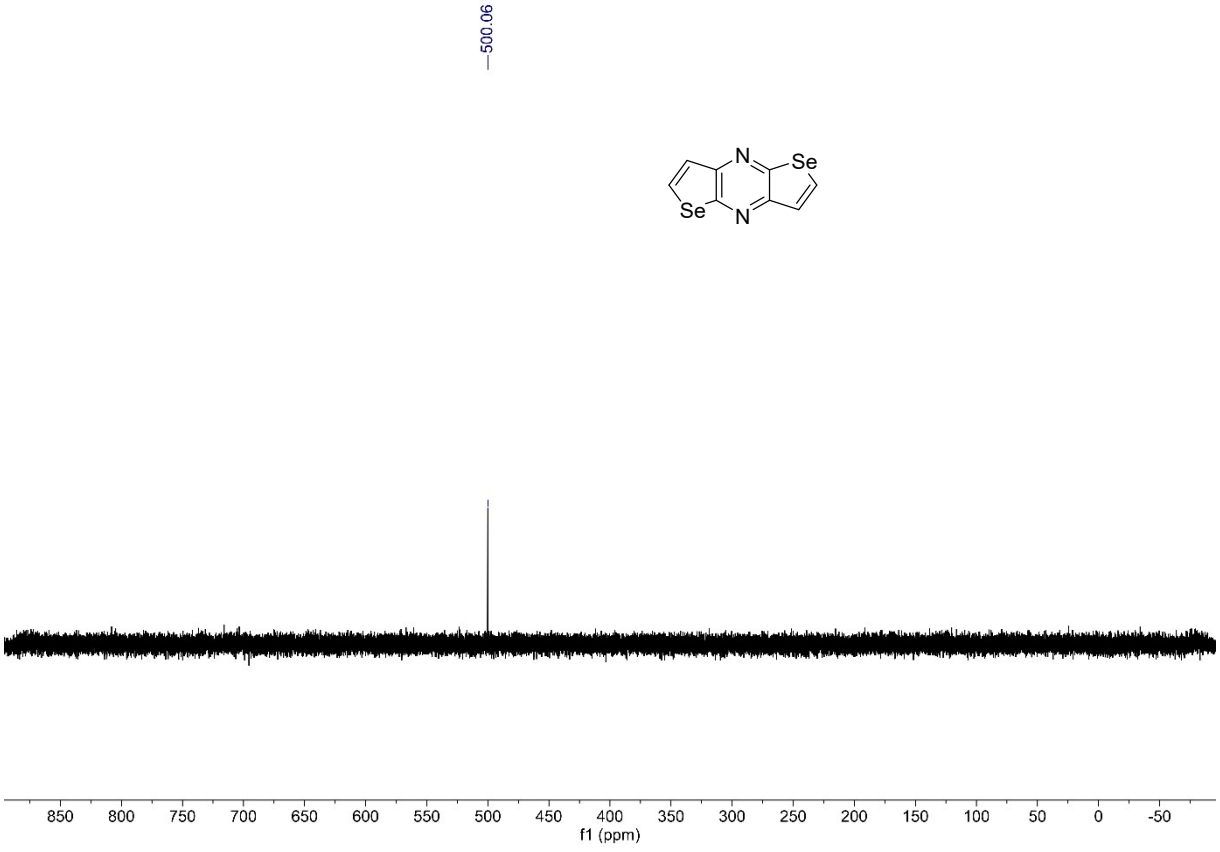

Figure S8. $^{77}Se\{^{1}H\}$ NMR spectrum (76 MHz, $CDCl_3$) of **3b**.

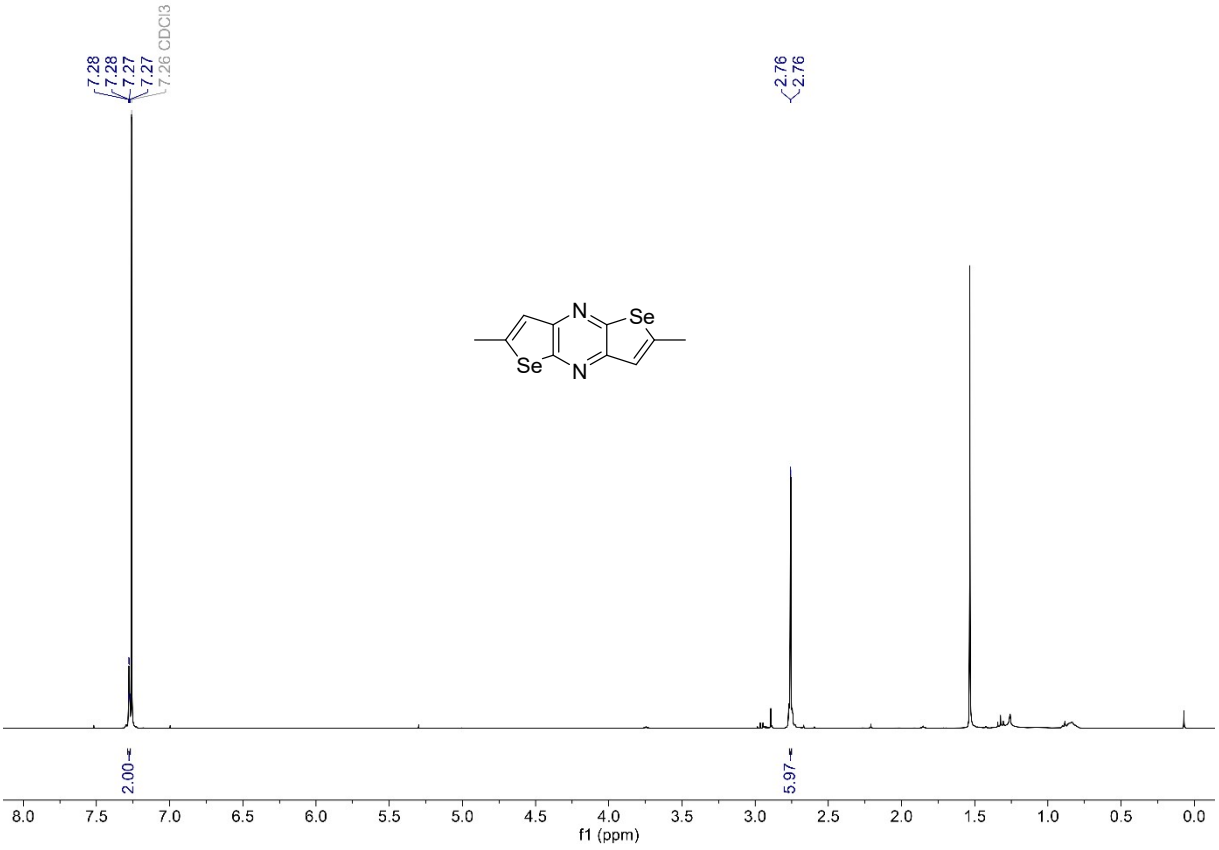

Figure S9. ^{1}H NMR spectrum (400 MHz, $CDCl_3$) of **3c**.

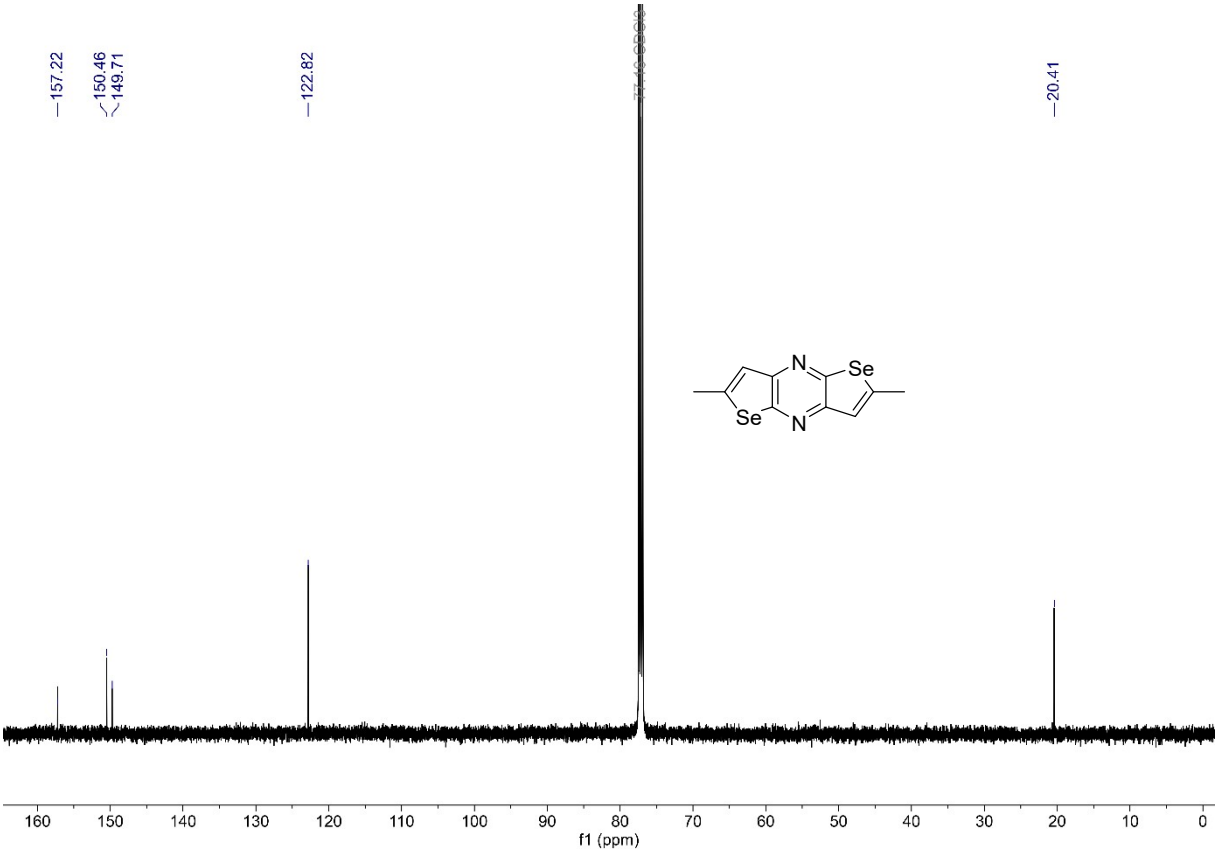

Figure S10. $^{13}C\{^{1}H\}$ NMR spectrum (101 MHz, $CDCl_3$) of **3c**.

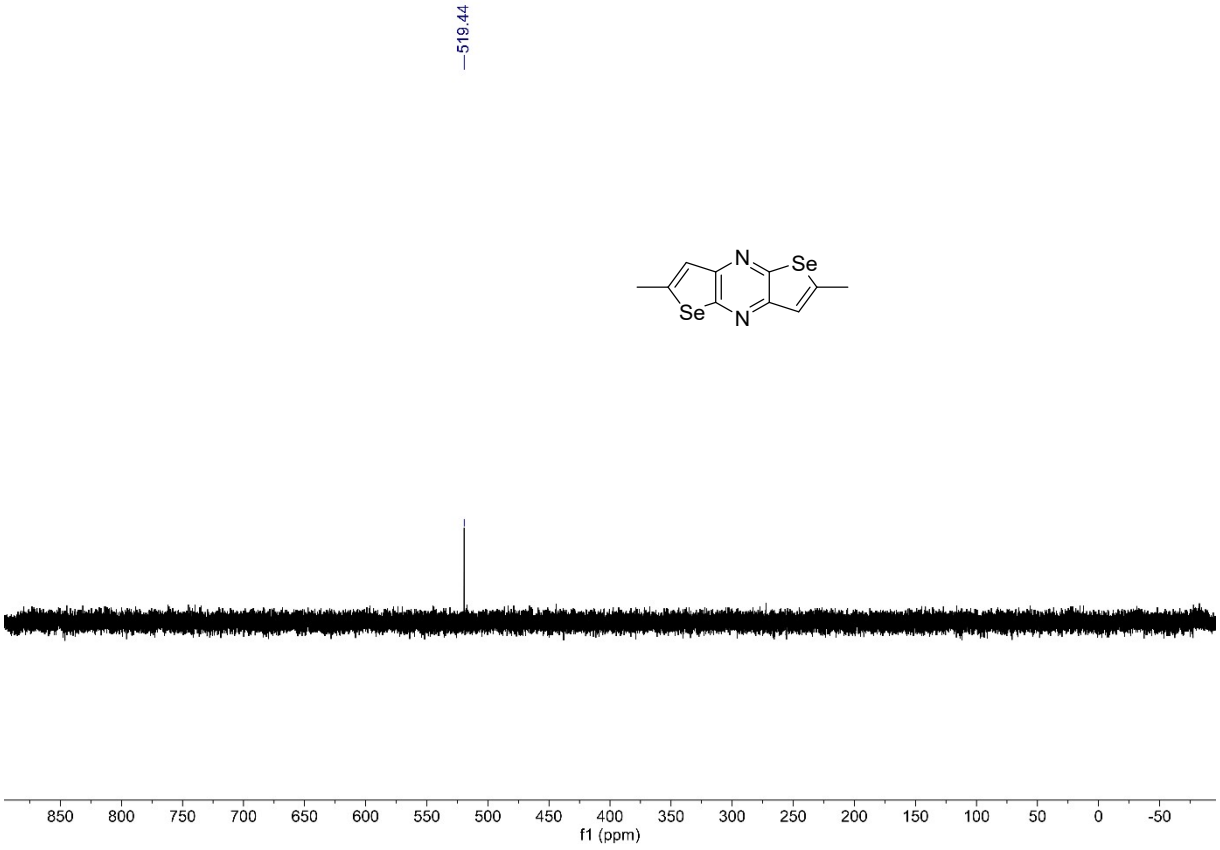

Figure S11. $^{77}Se\{^{1}H\}$ NMR spectrum (76 MHz, $CDCl_3$) of **3c**.

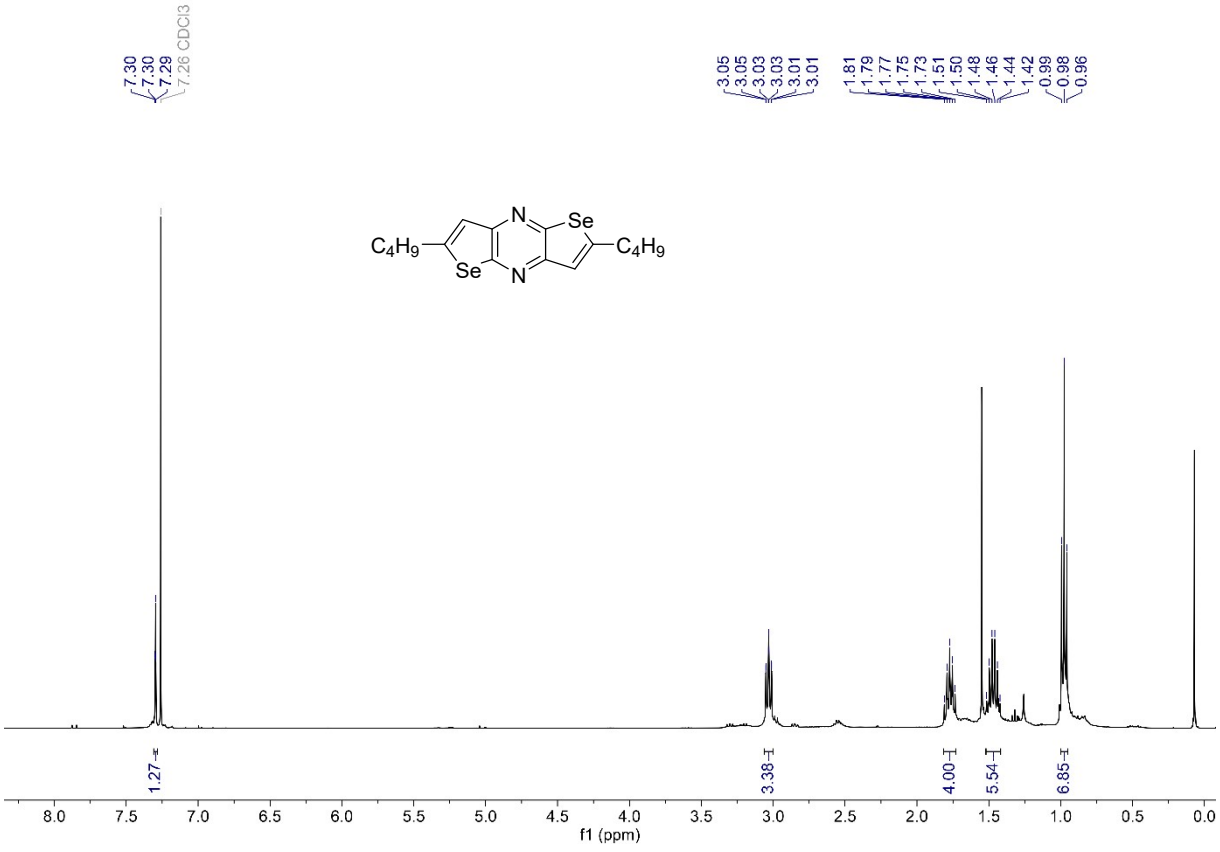

Figure S12. ^{1}H NMR spectrum (400 MHz, $CDCl_3$) of **3d**.

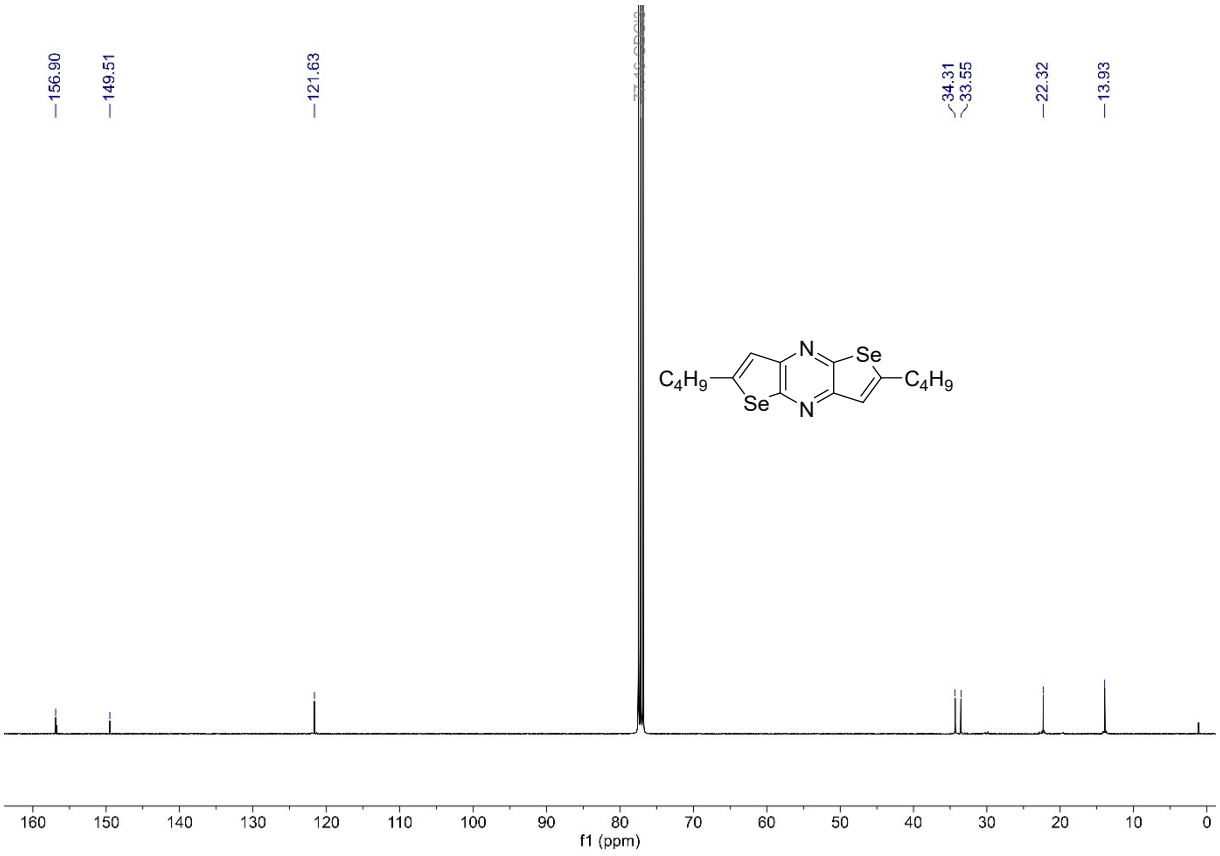

Figure S13. $^{13}C\{^{1}H\}$ NMR spectrum (101 MHz, $CDCl_3$) of **3d**.

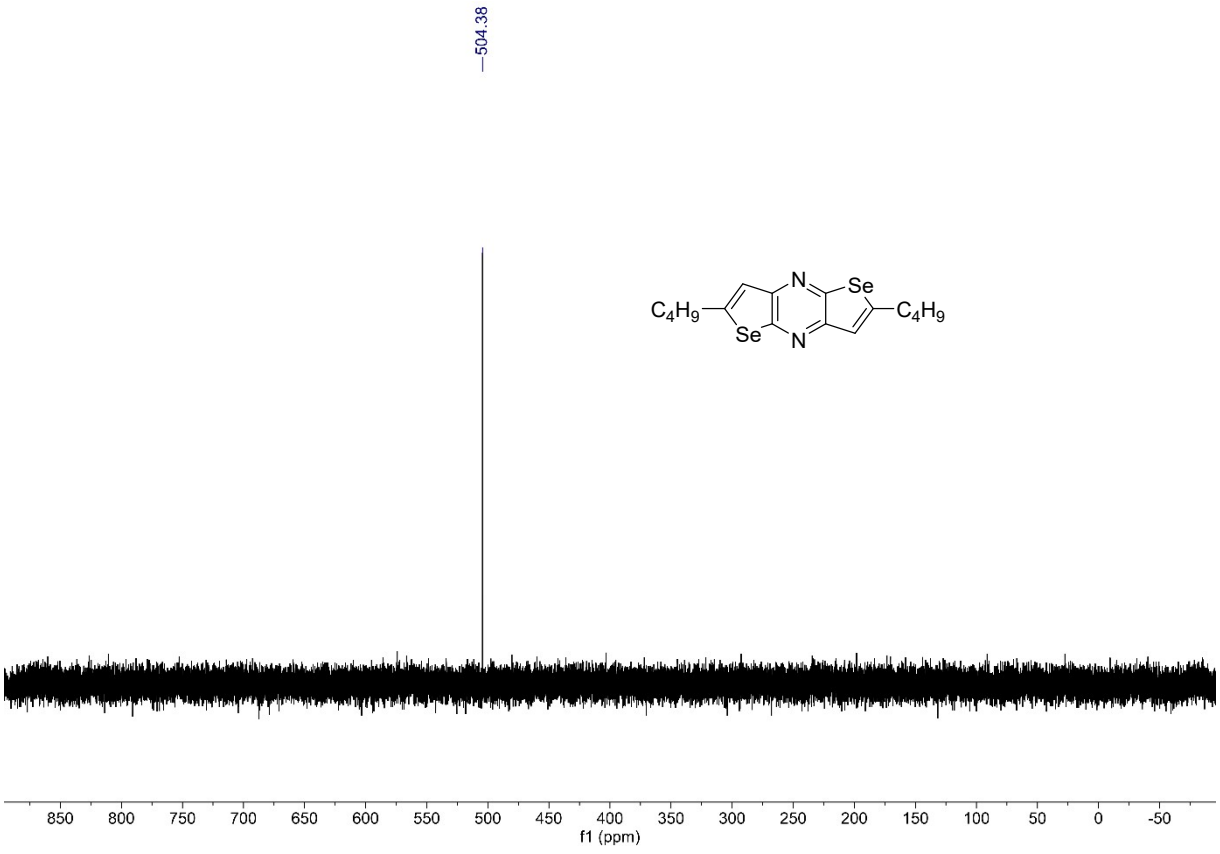

Figure S14. $^{77}Se\{^{1}H\}$ NMR spectrum (76 MHz, $CDCl_3$) of **3d**.

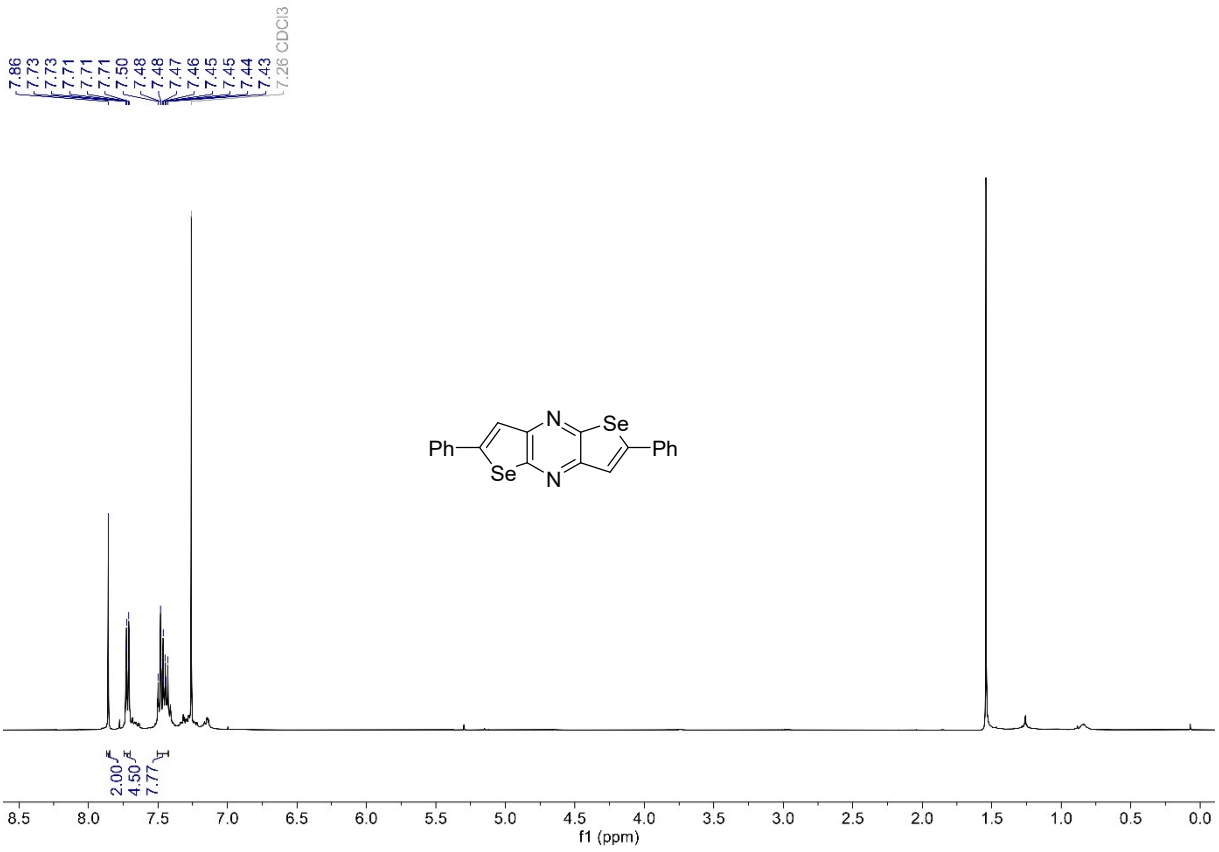

Figure S15. ^{1}H NMR spectrum (400 MHz, $CDCl_3$) of **3e**.

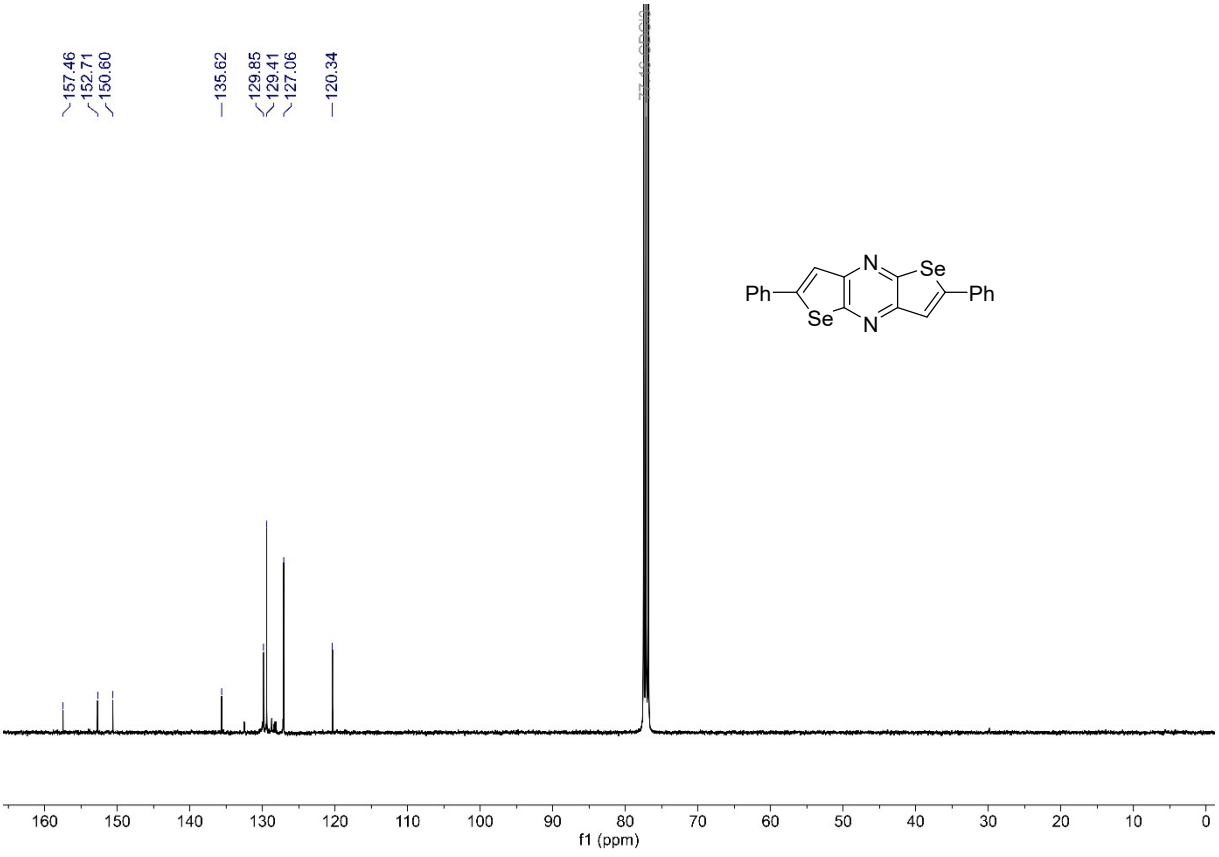

Figure S16. $^{13}C\{^{1}H\}$ NMR spectrum (101 MHz, $CDCl_3$) of **3e**.

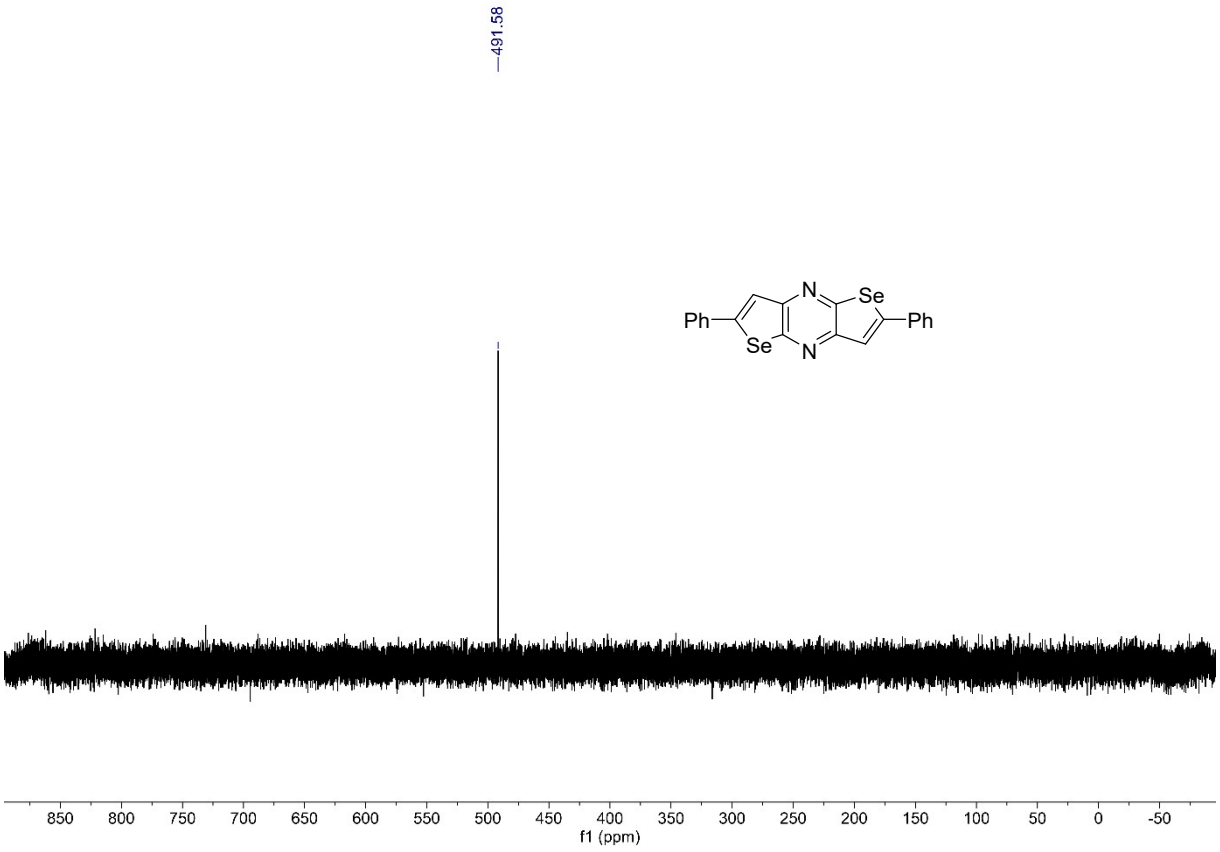

Figure S17. $^{77}Se\{^{1}H\}$ NMR spectrum (76 MHz, $CDCl_3$) of **3e**.

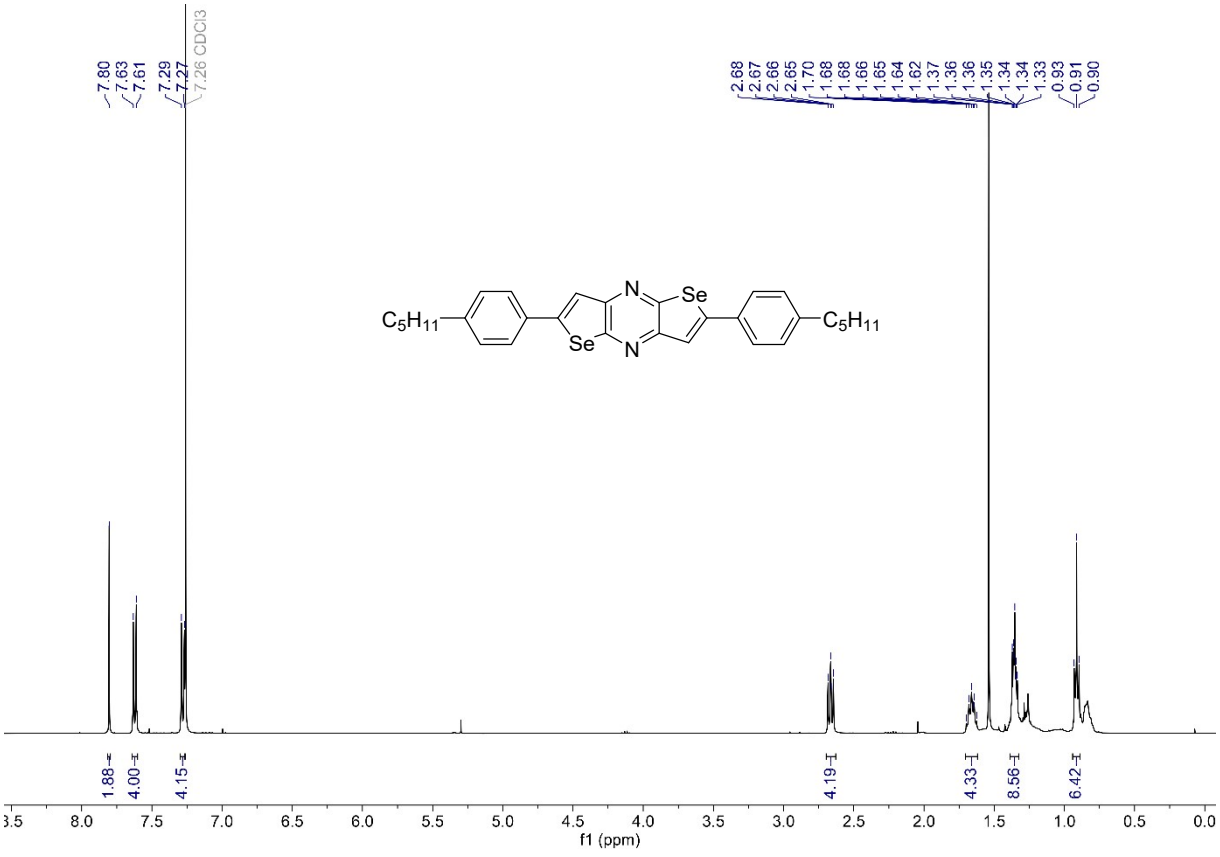

Figure S18. ^{1}H NMR spectrum (400 MHz, $CDCl_3$) of **3f**.

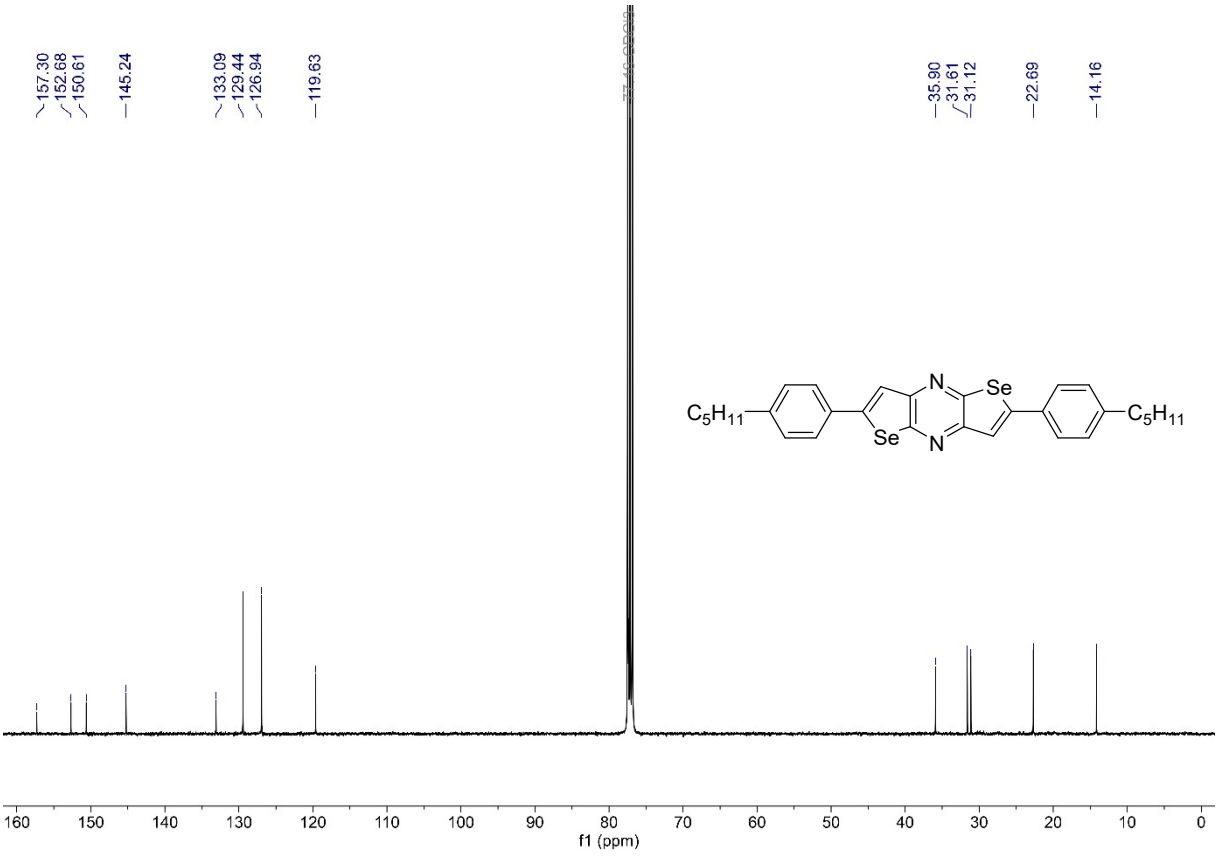

Figure S19. $^{13}C\{^{1}H\}$ NMR spectrum (101 MHz, $CDCl_3$) of **3f**.

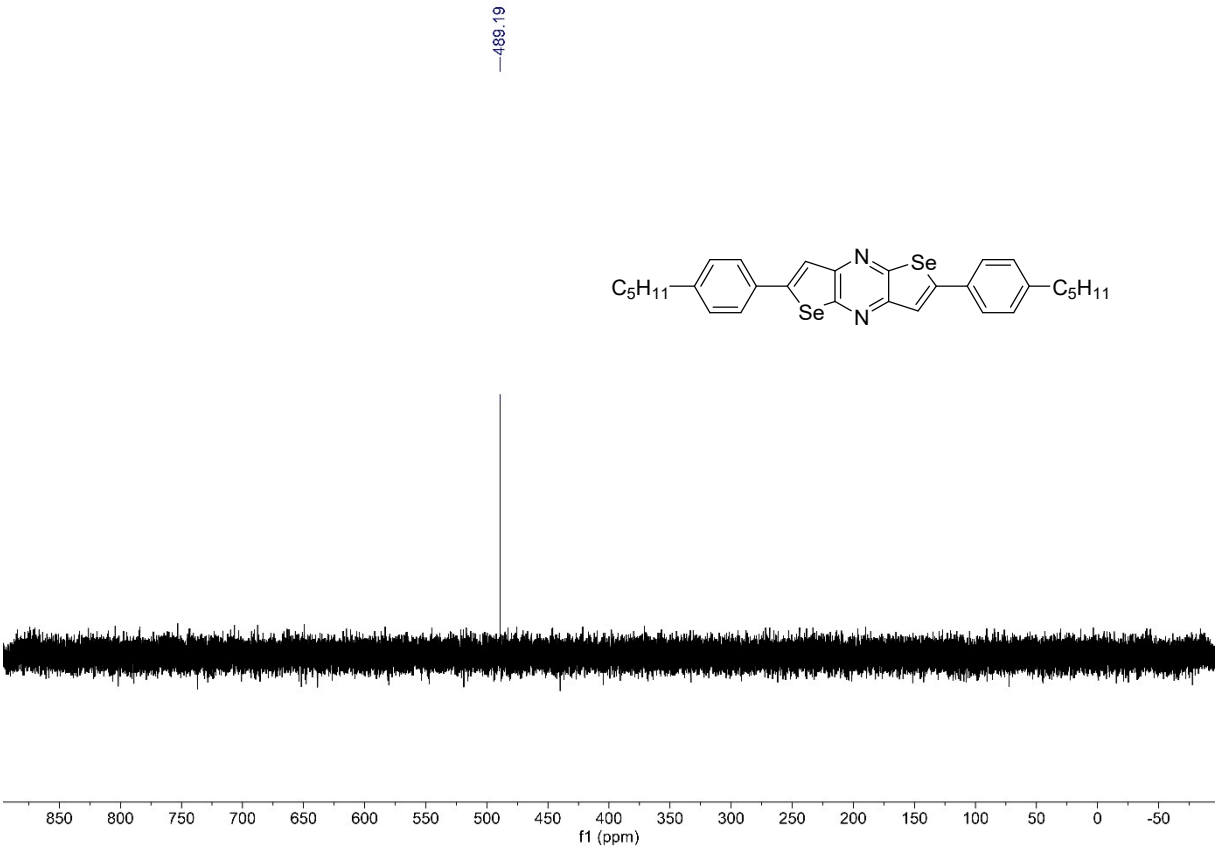

Figure S20. $^{77}Se\{^{1}H\}$ NMR spectrum (76 MHz, $CDCl_3$) of **3f**.

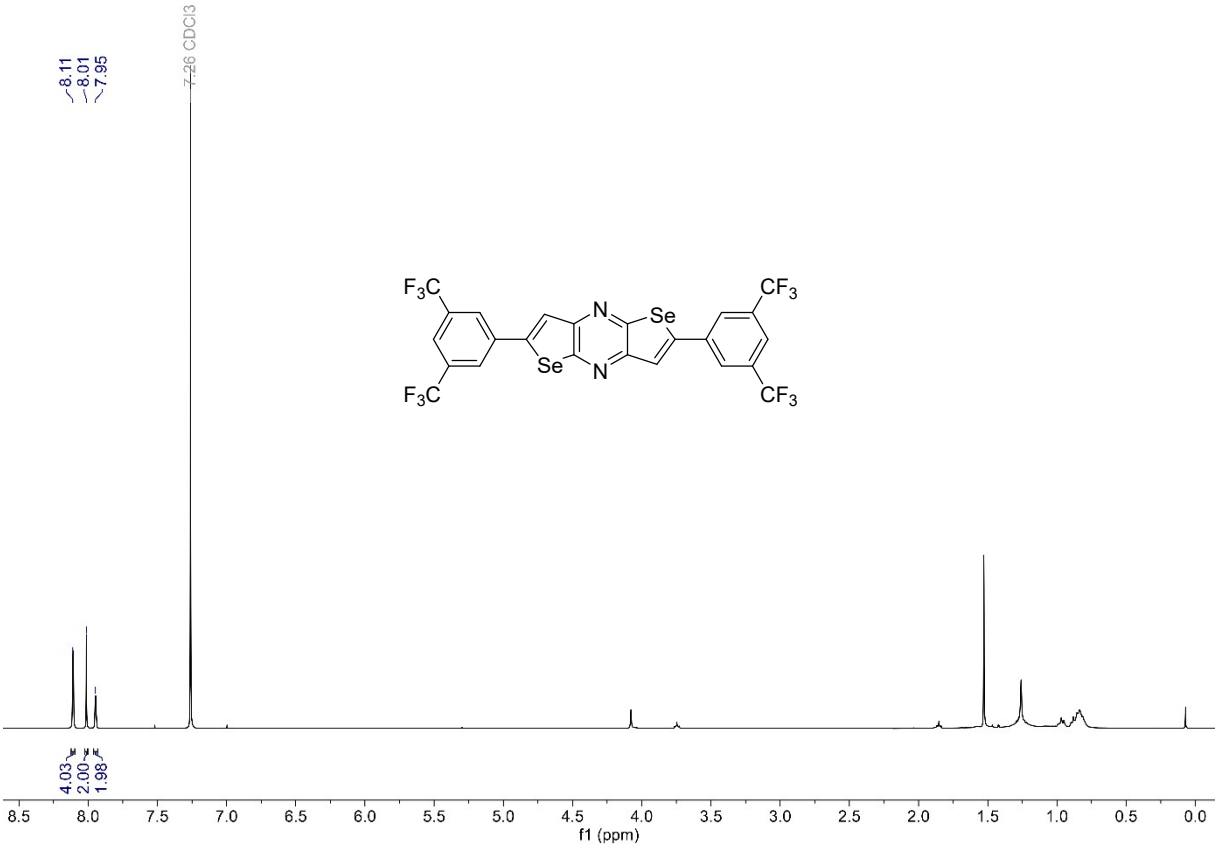

Figure S21. ^{1}H NMR spectrum (400 MHz, $CDCl_3$) of **3g**.

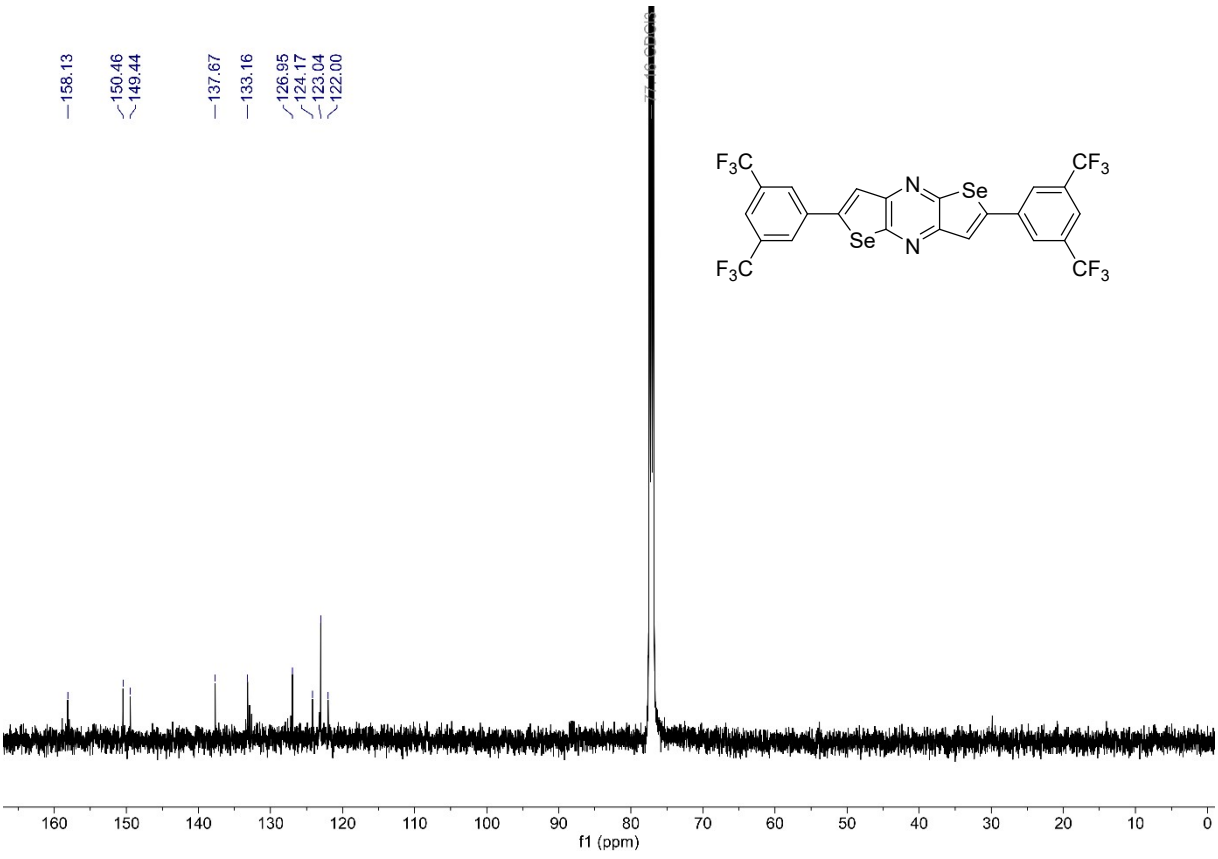

Figure S22. $^{13}C\{^{1}H\}$ NMR spectrum (101 MHz, $CDCl_3$) of **3g**.

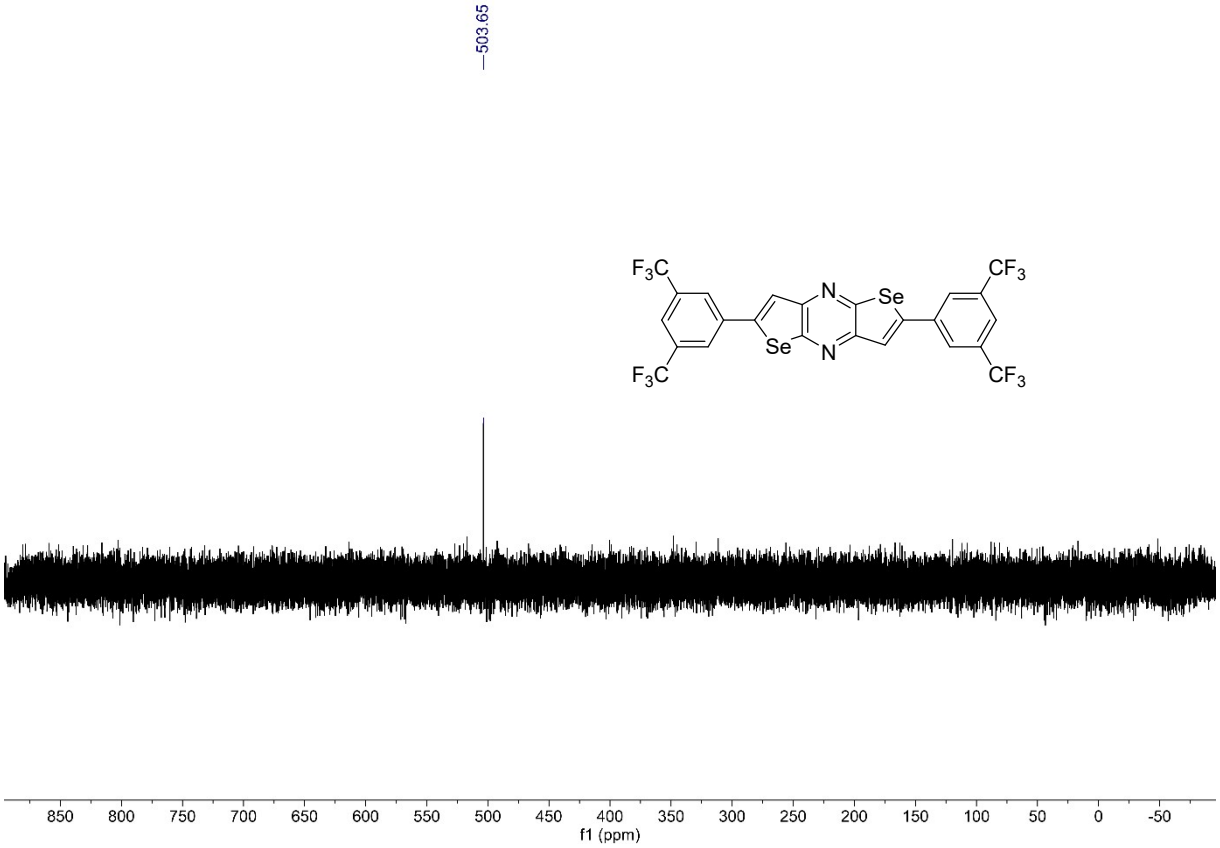

Figure S23. $^{77}Se\{^{1}H\}$ NMR spectrum (76 MHz, $CDCl_3$) of **3g**.

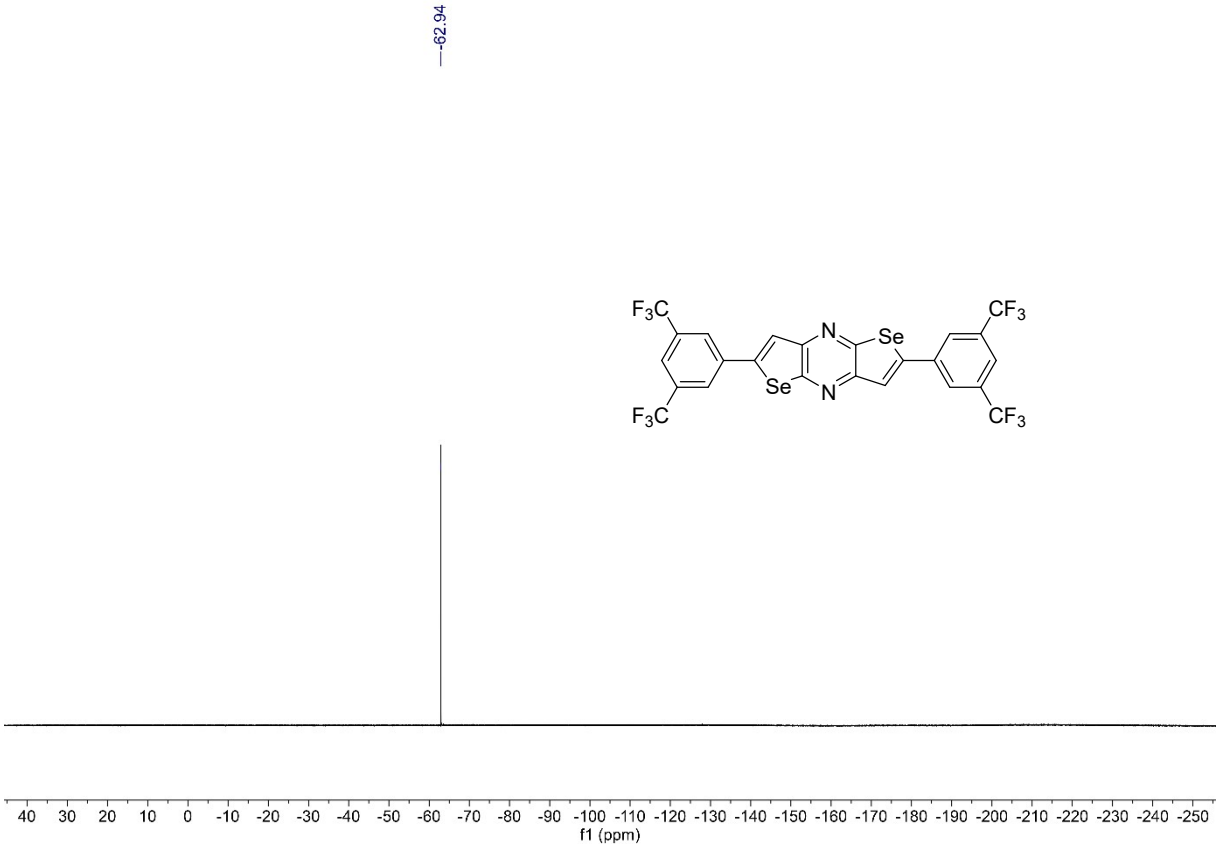

Figure S24. $^{19}F\{^{1}H\}$ NMR spectrum (283 MHz, $CDCl_3$) of **3g**.

3 UV-Vis and Fluorescence Spectra

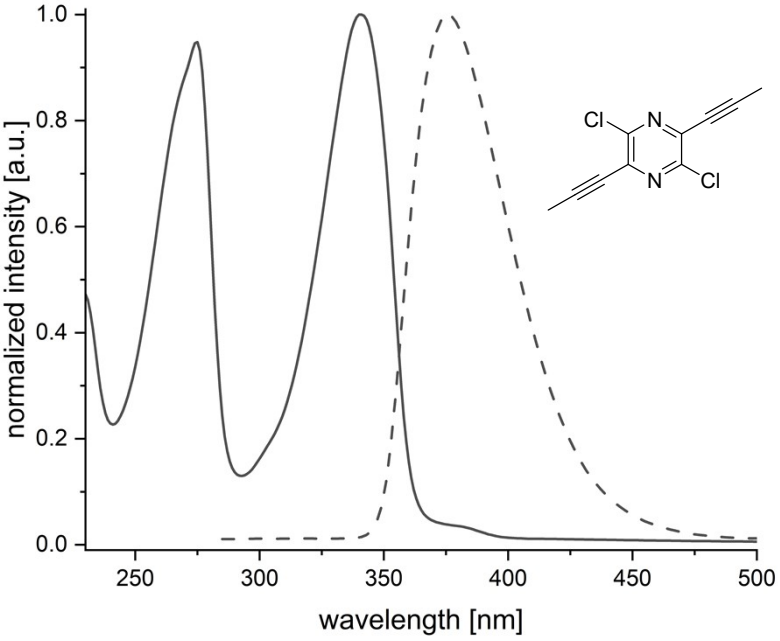

Figure S25. Absorption (solid line) and emission (dashed line) spectra of **2c** in DCM.

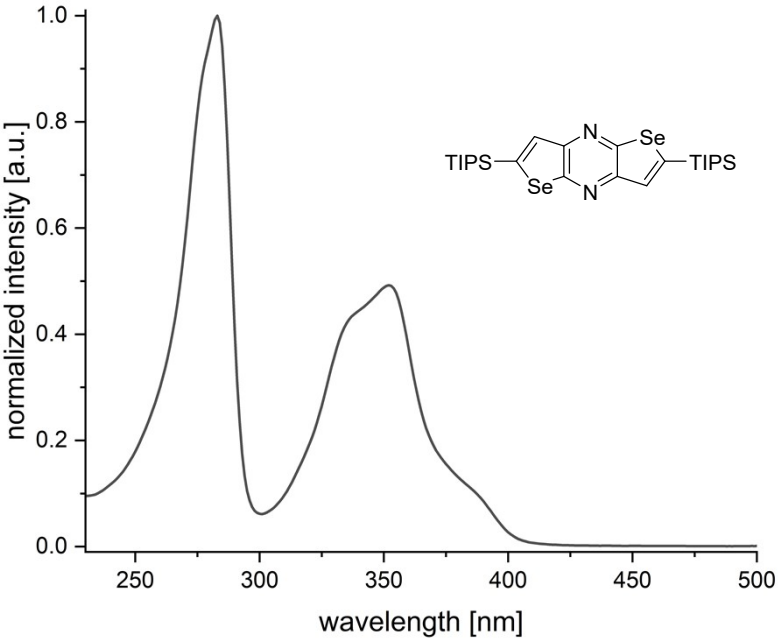

Figure S26. Absorption spectrum of **3a** in DCM.

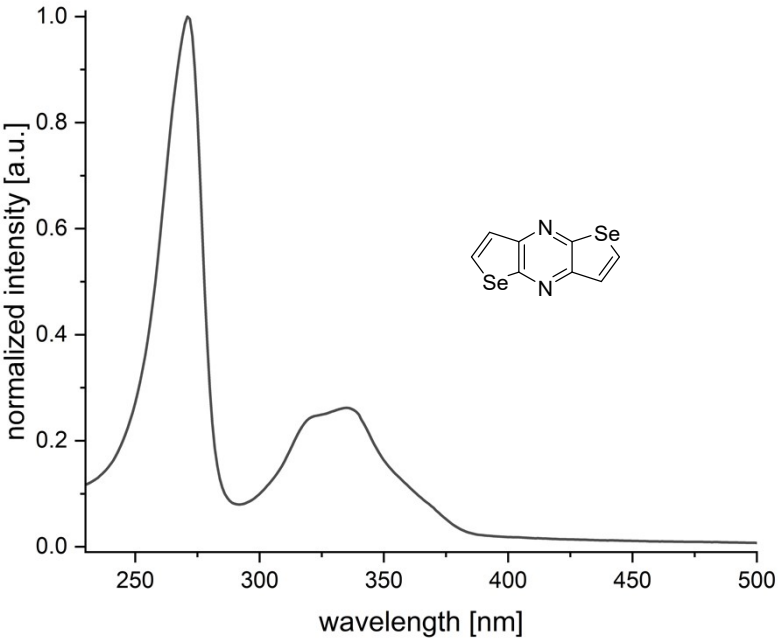

Figure S27. Absorption spectrum of **3b** in DCM.

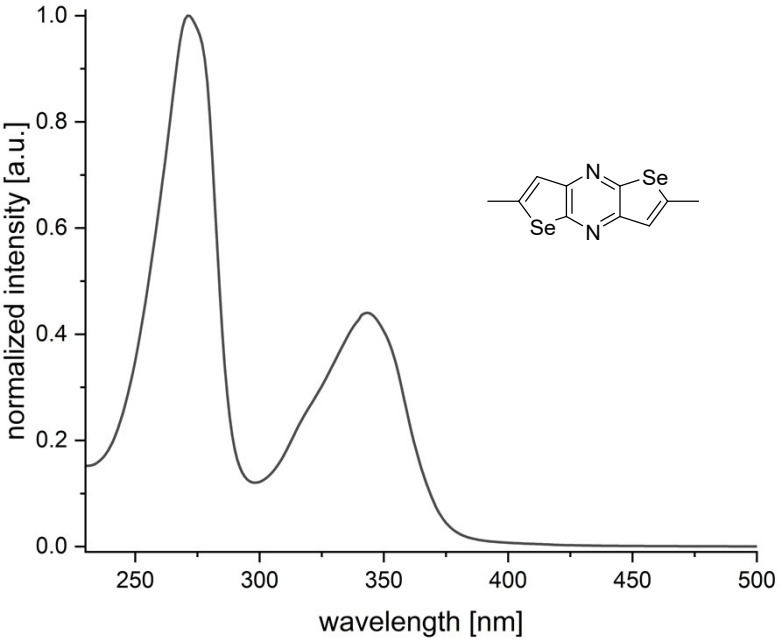

Figure S28. Absorption spectrum of **3c** in DCM.

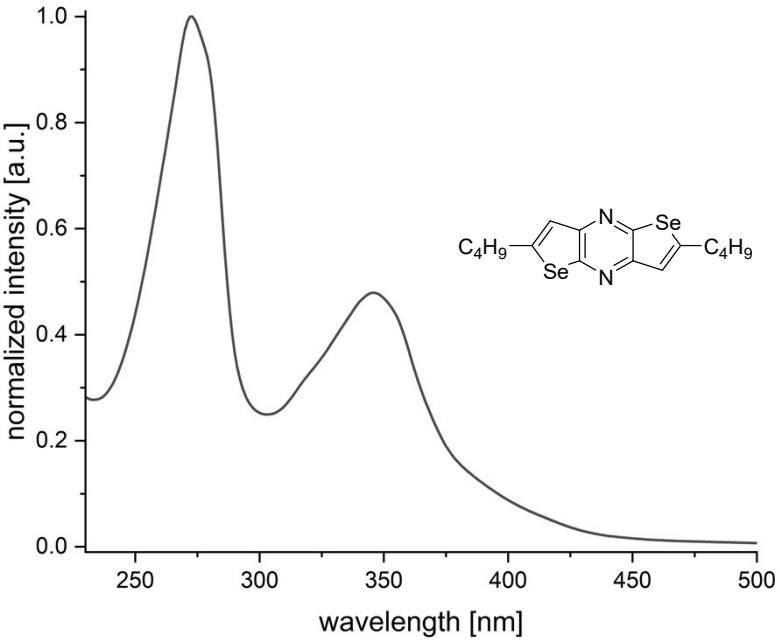

Figure S29. Absorption spectrum of **3d** in DCM.

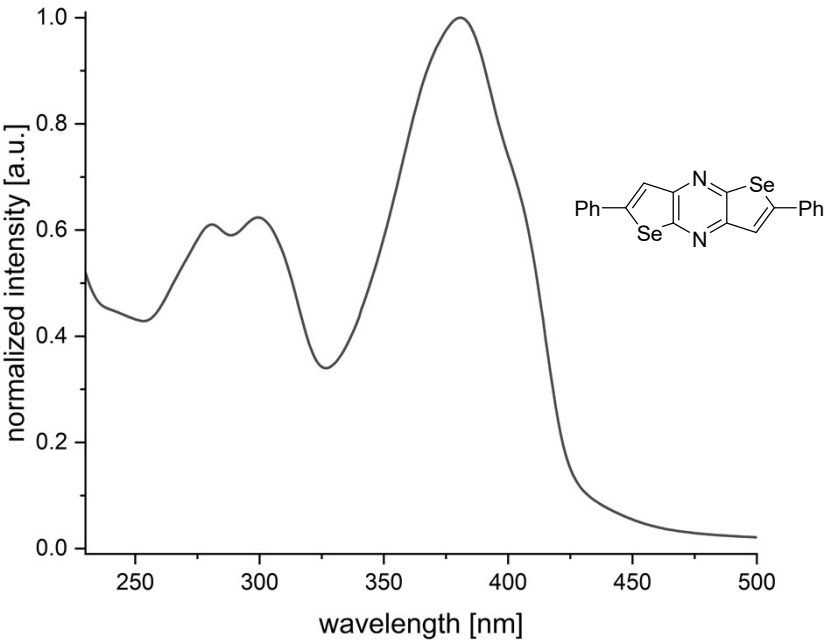

Figure S30. Absorption spectrum of **3e** in DCM.

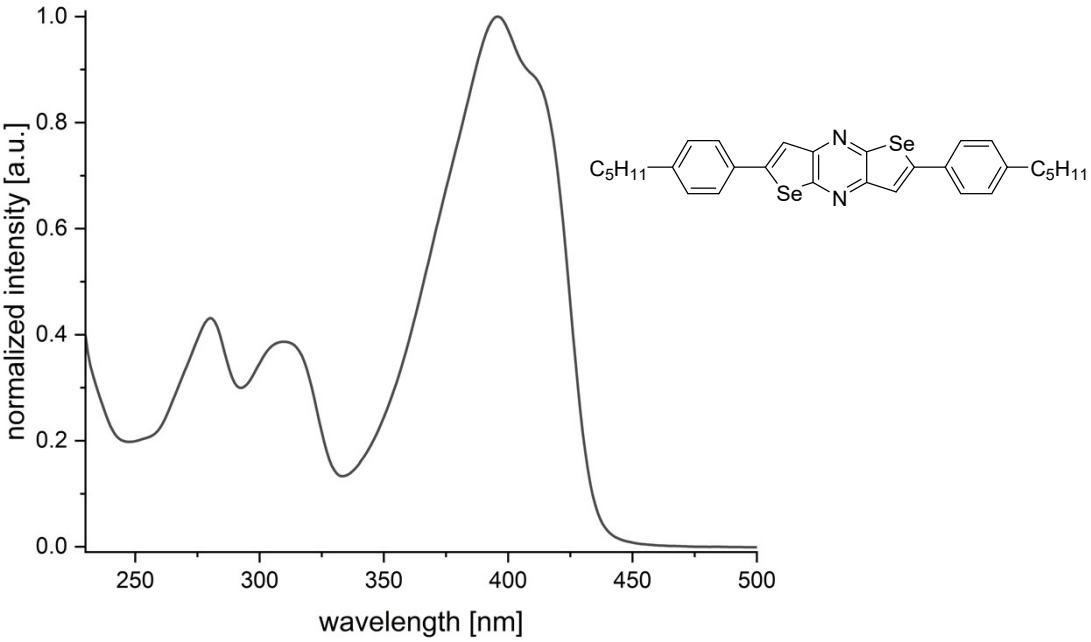

Figure S31. Absorption spectrum of **3f** in DCM.

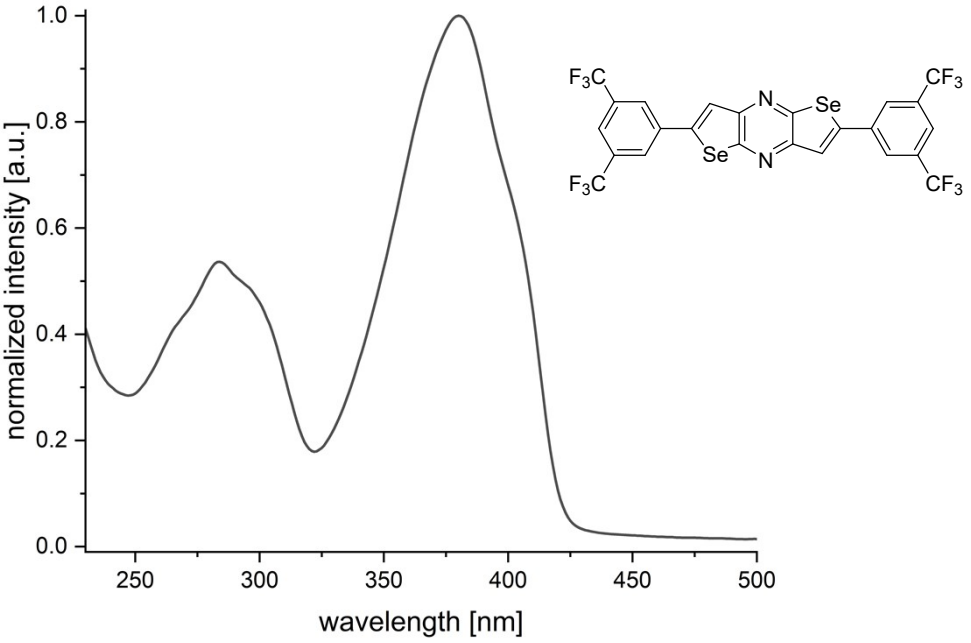

Figure S32. Absorption spectrum of **3g** in DCM.

4 Electrochemical Data

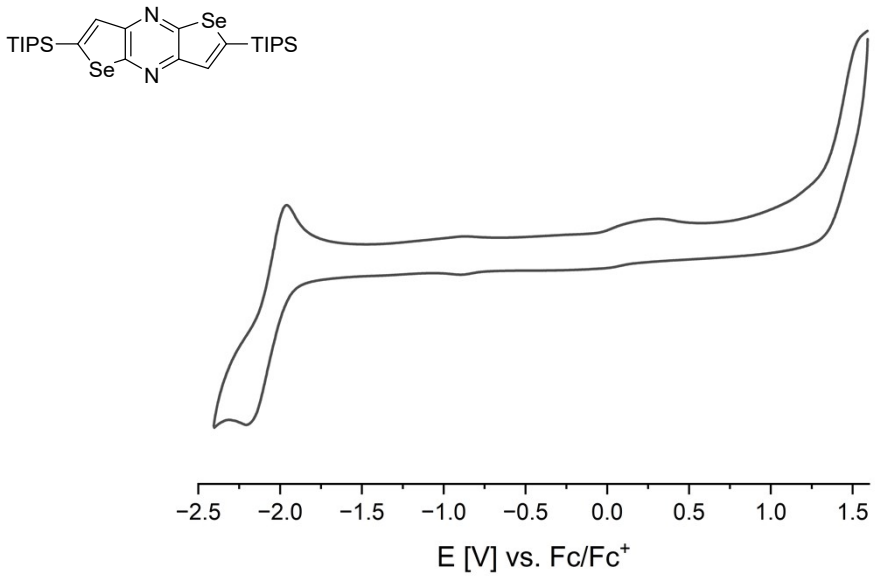

Figure S33. Cyclic voltammogram of **3a** in DCM/tetrabutylammonium hexafluorophosphate (0.1 M), scan speed 500 mV/s at r.t.

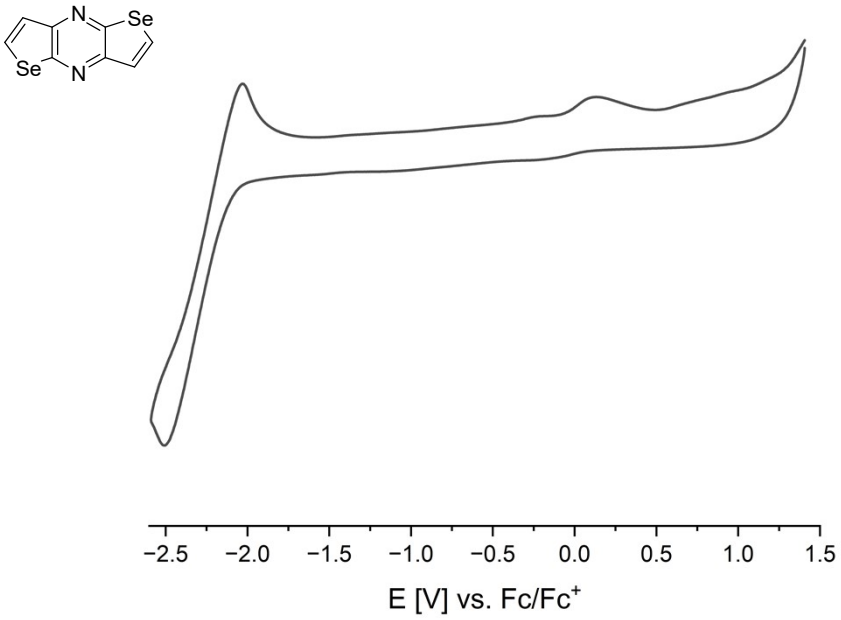

Figure S34. Cyclic voltammogram of **3b** in DCM/tetrabutylammonium hexafluorophosphate (0.1 M), scan speed 500 mV/s at r.t.

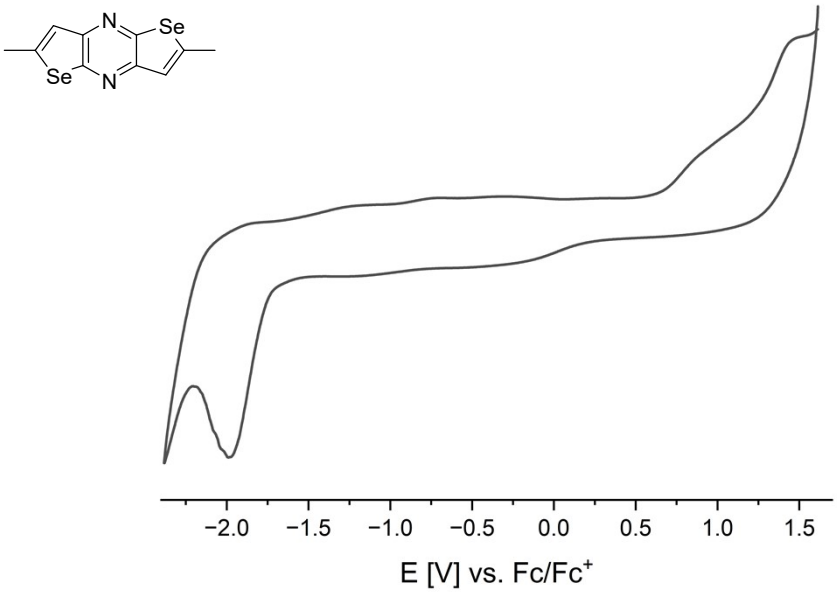

Figure S35. Cyclic voltammogram of **3c** in DCM/tetrabutylammonium hexafluorophosphate (0.1 M), scan speed 500 mV/s at r.t.

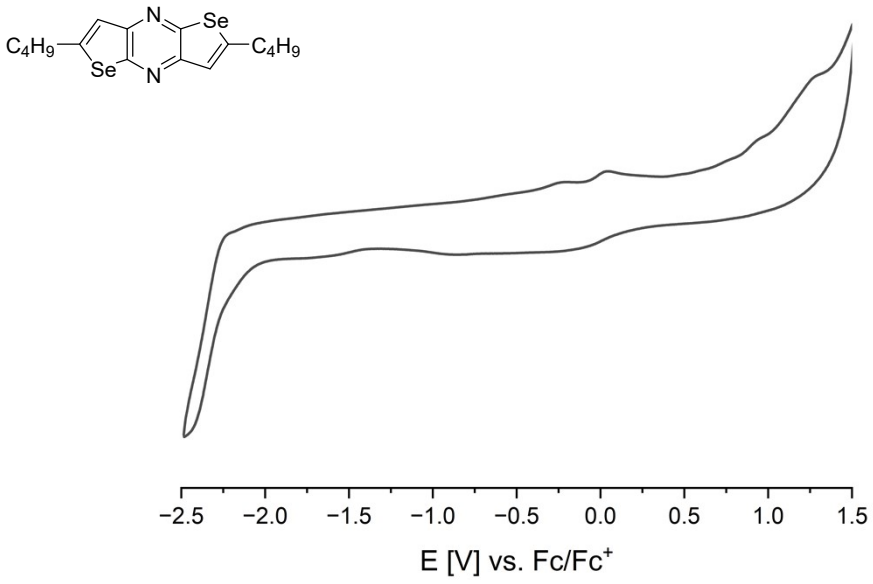

Figure S36. Cyclic voltammogram of **3d** in DCM/tetrabutylammonium hexafluorophosphate (0.1 M), scan speed 500 mV/s at r.t.

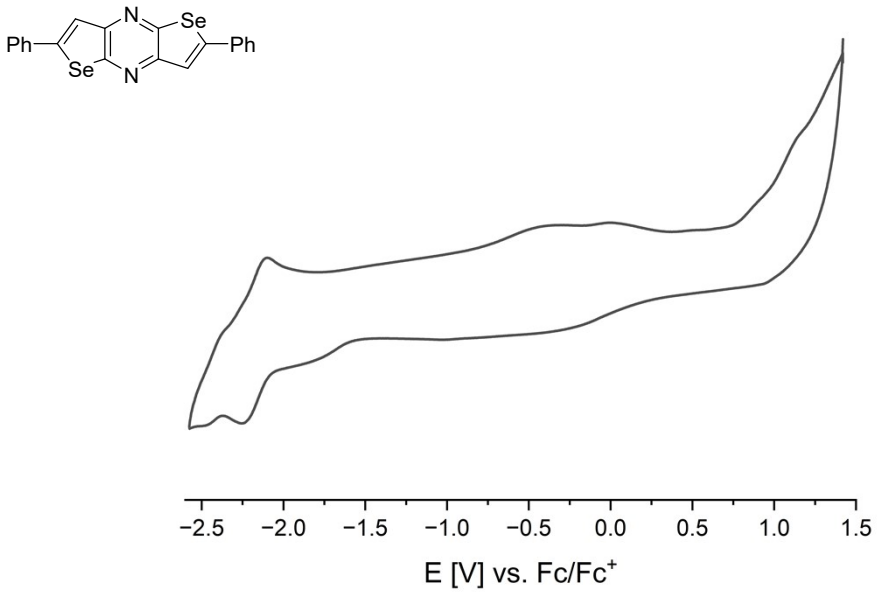

Figure S37. Cyclic voltammogram of **3e** in DCM/tetrabutylammonium hexafluorophosphate (0.1 M), scan speed 500 mV/s at r.t.

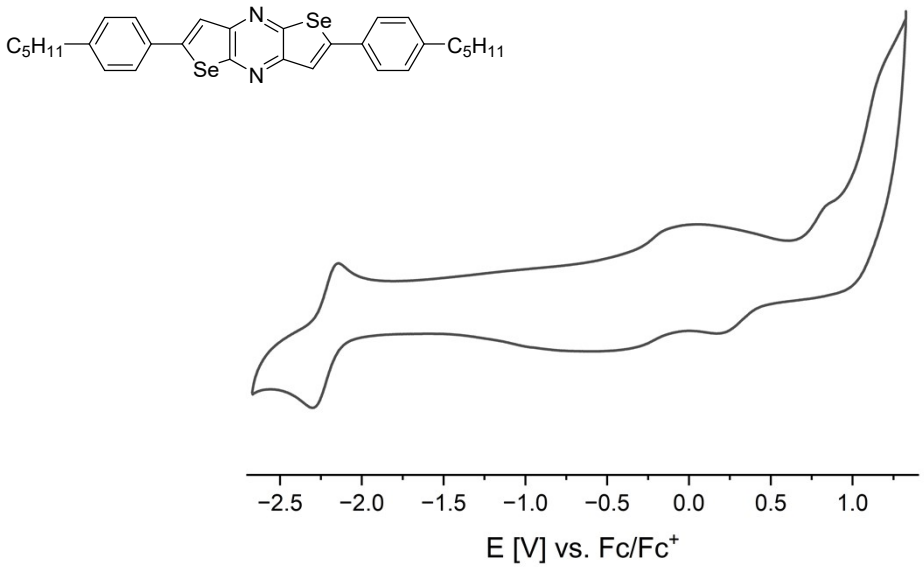

Figure S38. Cyclic voltammogram of **3f** in DCM/tetrabutylammonium hexafluorophosphate (0.1 M), scan speed 500 mV/s at r.t.

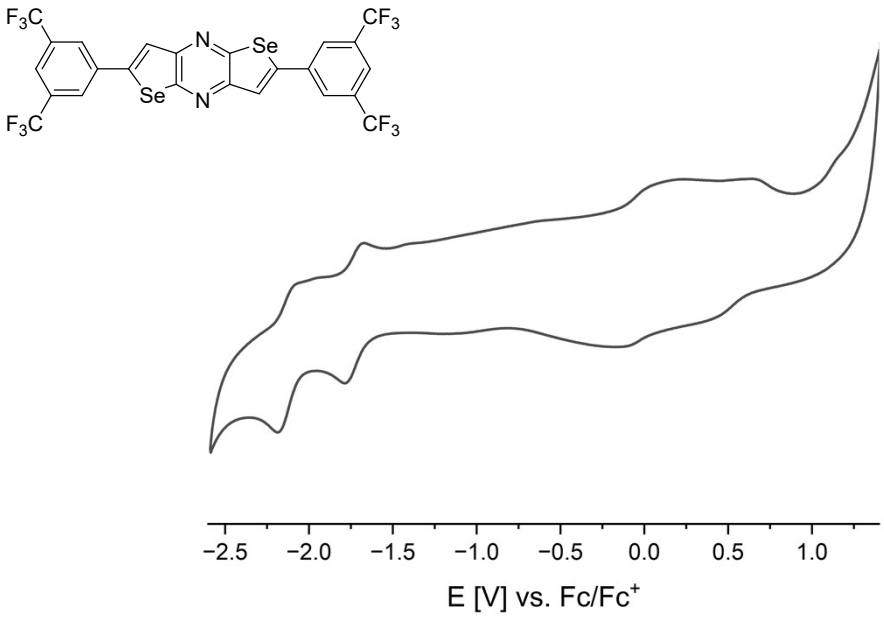

Figure S39. Cyclic voltammogram of **3g** in DCM/tetrabutylammonium hexafluorophosphate (0.1 M), scan speed 500 mV/s at r.t.

5 Crystallographic Data

Table S1. Crystal structure, crystal data and structure refinement of **2a** (CCDC 2313523).

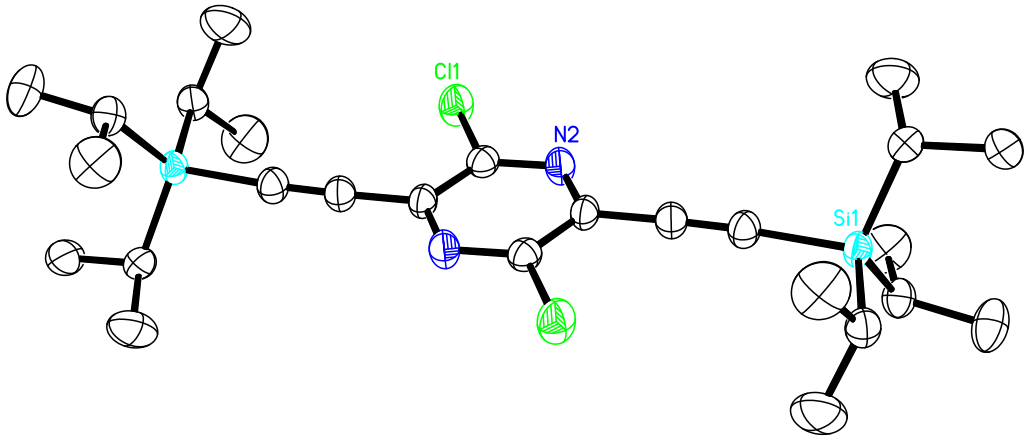

Empirical formula	$C_{26}H_{42}Cl_2N_2Si_2$	
Formula weight	509.69	
Temperature	200(2) K	
Wavelength	0.71073 Å	
Crystal system	monoclinic	
Space group	I2/m	
Z	2	
Unit cell dimensions	a = 10.530(2) Å	α = 90 deg.
	b = 10.929(2) Å	β = 96.525(4) deg.
	c = 12.931(4) Å	γ = 90 deg.
Volume	1478.5(6) $Å^3$	
Density (calculated)	1.14 g/cm^3	
Absorption coefficient	0.32 mm^{-1}	
Crystal shape	plate	
Crystal size	0.106 x 0.060 x 0.016 mm^3	
Crystal colour	colourless	
Theta range for data collection	2.4 to 26.7 deg.	
Index ranges	-13≤h≤13, -13≤k≤13, -16≤l≤16	
Reflections collected	7854	
Independent reflections	1638 (R(int) = 0.1057)	
Observed reflections	1016 (I > 2σ(I))	
Absorption correction	Semi-empirical from equivalents	
Max. and min. transmission	0.96 and 0.86	
Refinement method	Full-matrix least-squares on F^2	
Data/restraints/parameters	1638 / 0 / 88	
Goodness-of-fit on F^2	1.03	
Final R indices (I>2sigma(I))	R1 = 0.066, wR2 = 0.101	
Largest diff. peak and hole	0.27 and -0.31 $eÅ^{-3}$	

Table S2. Crystal structure, crystal data and structure refinement of **2c** (CCDC 2313524).

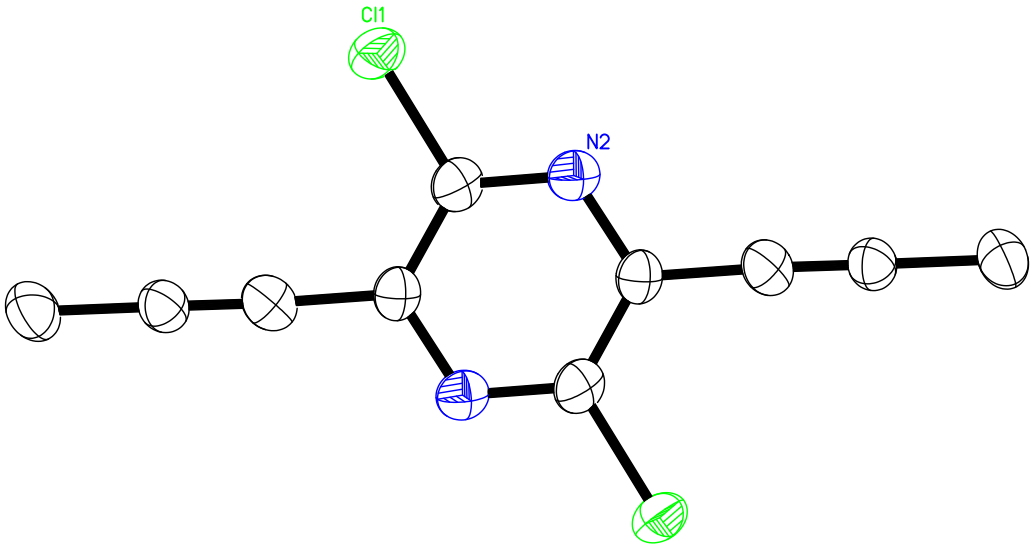

Empirical formula	$C_{10}H_6Cl_2N_2$	
Formula weight	225.07	
Temperature	200(2) K	
Wavelength	0.71073 Å	
Crystal system	monoclinic	
Space group	$P2_1/n$	
Z	2	
Unit cell dimensions	a = 8.833(11) Å	α = 90 deg.
	b = 4.114(5) Å	β =106.095(14) deg.
	c = 14.134(17) Å	γ = 90 deg.
Volume	493.5(11) $Å^3$	
Density (calculated)	1.51 g/cm^3	
Absorption coefficient	0.61 mm^{-1}	
Crystal shape	plate	
Crystal size	0.192 x 0.042 x 0.015 mm^3	
Crystal colour	brown	
Theta range for data collection	2.5 to 27.6 deg.	
Index ranges	$-11 \le h \le 11$, $-5 \le k \le 4$, $-18 \le l \le 18$	
Reflections collected	3053	
Independent reflections	1059 (R(int) = 0.0752)	
Observed reflections	684 ($I > 2\sigma(I)$)	
Absorption correction	Semi-empirical from equivalents	
Max. and min. transmission	0.96 and 0.78	
Refinement method	Full-matrix least-squares on F^2	
Data/restraints/parameters	1059 / 0 / 65	
Goodness-of-fit on F^2	1.04	
Final R indices (I>2sigma(I))	R1 = 0.077, wR2 = 0.190	
Largest diff. peak and hole	0.53 and -0.50 $eÅ^{-3}$	

Table S3. Crystal structure, crystal data and structure refinement of **3a** (CCDC 2313525).

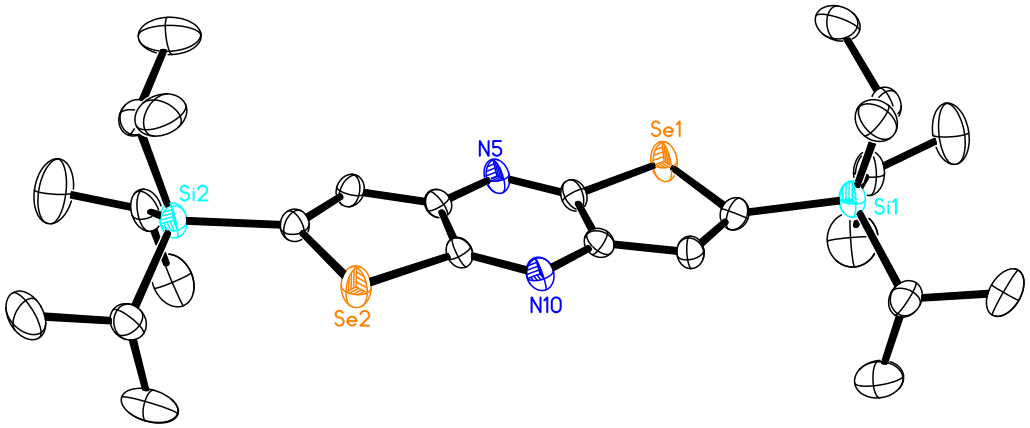

Empirical formula	$C_{26}H_{44}N_2Se_2Si_2$	
Formula weight	598.73	
Temperature	200(2) K	
Wavelength	0.71073 Å	
Crystal system	monoclinic	
Space group	$P2_1/c$	
Z	4	
Unit cell dimensions	a = 14.4080(14) Å	α = 90 deg.
	b = 16.0163(16) Å	β = 97.694(2) deg.
	c = 12.9816(13) Å	γ = 90 deg.
Volume	2968.7(5) $Å^3$	
Density (calculated)	1.34 g/cm^3	
Absorption coefficient	2.59 mm^{-1}	
Crystal shape	plate	
Crystal size	0.160 x 0.057 x 0.010 mm^3	
Crystal colour	yellow	
Theta range for data collection	1.4 to 28.2 deg.	
Index ranges	$-18\leq h\leq 18$, $-21\leq k\leq 21$, $-17\leq l\leq 16$	
Reflections collected	33573	
Independent reflections	7194 (R(int) = 0.1121)	
Observed reflections	3804 ($I > 2\sigma(I)$)	
Absorption correction	Semi-empirical from equivalents	
Max. and min. transmission	0.96 and 0.85	
Refinement method	Full-matrix least-squares on F^2	
Data/restraints/parameters	7194 / 0 / 301	
Goodness-of-fit on F^2	0.99	
Final R indices (I>2sigma(I))	R1 = 0.050, wR2 = 0.079	
Largest diff. peak and hole	0.45 and -0.46 $eÅ^{-3}$	

Table S4. Crystal structure, crystal data and structure refinement of **3b** (CCDC 2313526).

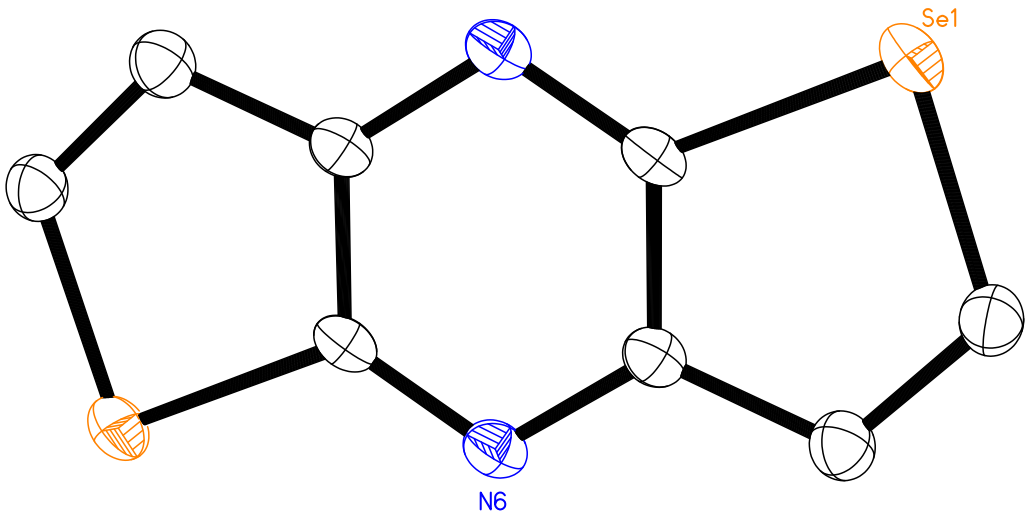

Empirical formula	$C_8H_4N_2Se_2$
Formula weight	286.05
Temperature	200(2) K
Wavelength	0.71073 Å
Crystal system	monoclinic
Space group	$P2_1/n$
Z	2
Unit cell dimensions	a = 4.1984(7) Å α = 90 deg.
	b = 8.1335(12) Å β = 96.9877(19) deg.
	c = 12.0157(18) Å γ = 90 deg.
Volume	407.26(11) $Å^3$
Density (calculated)	2.33 g/cm^3
Absorption coefficient	9.01 mm^{-1}
Crystal shape	plank
Crystal size	0.187 x 0.046 x 0.013 mm^3
Crystal colour	brown
Theta range for data collection	3.0 to 30.2 deg.
Index ranges	$-5\leq h\leq 5$, $-11\leq k\leq 11$, $-16\leq l\leq 16$
Reflections collected	4782
Independent reflections	1120 (R(int) = 0.0275)
Observed reflections	969 ($I > 2\sigma(I)$)
Absorption correction	Semi-empirical from equivalents
Max. and min. transmission	0.75 and 0.45
Refinement method	Full-matrix least-squares on F^2
Data/restraints/parameters	1120 / 0 / 55
Goodness-of-fit on F^2	1.11
Final R indices (I>2sigma(I))	R1 = 0.023, wR2 = 0.056
Largest diff. peak and hole	0.48 and -0.37 $eÅ^{-3}$

Table S5. Crystal structure, crystal data and structure refinement of **3f** (CCDC 2313527).

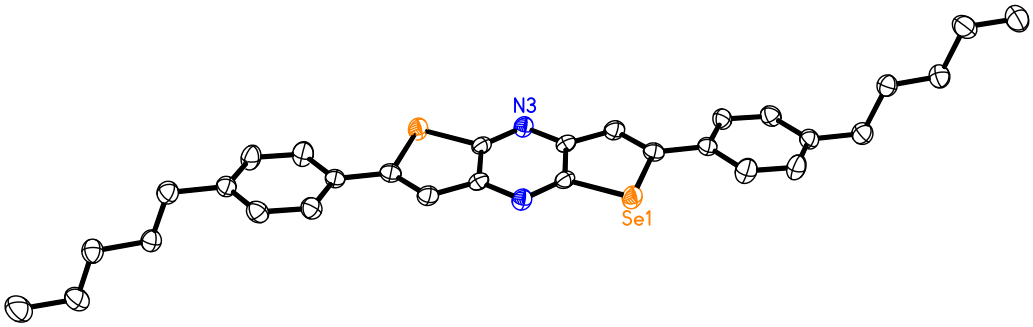

Empirical formula	$C_{30}H_{32}N_2Se_2$	
Formula weight	578.49	
Temperature	200(2) K	
Wavelength	0.71073 Å	
Crystal system	triclinic	
Space group	$P\bar{1}$	
Z	1	
Unit cell dimensions	a = 4.7908(6) Å	α = 75.701(4) deg.
	b = 9.1049(13) Å	β = 89.134(3) deg.
	c = 15.3497(18) Å	γ = 80.513(3) deg.
Volume	639.70(14) Å^3	
Density (calculated)	1.50 g/cm^3	
Absorption coefficient	2.91 mm^{-1}	
Crystal shape	plank	
Crystal size	0.392 x 0.029 x 0.019 mm^3	
Crystal colour	yellow	
Theta range for data collection	1.4 to 26.7 deg.	
Index ranges	$-6\leq h\leq 6$, $-11\leq k\leq 11$, $-19\leq l\leq 19$	
Reflections collected	11314	
Independent reflections	2689 (R(int) = 0.0945)	
Observed reflections	1875 ($I > 2\sigma(I)$)	
Absorption correction	Semi-empirical from equivalents	
Max. and min. transmission	0.96 and 0.71	
Refinement method	Full-matrix least-squares on F^2	
Data/restraints/parameters	2689 / 0 / 155	
Goodness-of-fit on F^2	1.01	
Final R indices (I>2sigma(I))	R1 = 0.047, wR2 = 0.072	
Largest diff. peak and hole	0.48 and -0.43 eÅ^{-3}	

6 Computational Investigation

6.1 Computational Details

All geometry optimizations, subsequent frequency analyses, and calculations concerning transition states were performed in the gas phase using Orca 5.0.3[5] on the bwForCluster Justus 2. The B3LYP[6-9] functional and the 6-311G(d,p)[10] basis set were employed.

6.2 Overview of the Computed Molecules

Table S6. Energies of all computed structures.

Compound	E_{HOMO} [eV]	E_{LUMO} [eV]	$E_{g(calc)}$ [eV]
3a	-5.96	-2.07	3.89
3b	-6.10	-2.06	4.11
3c	-5.99	-1.81	4.17
3d	-5.92	-1.78	4.14
3e	-5.80	-2.27	3.52
3f	-5.62	-2.15	3.47
3g	-6.51	-3.06	3.44

6.3 Coordinates of the Optimized Geometries

3a

xyz

0 1

6	-2.528687000	0.668802000	-0.192411000
6	-2.071732000	-0.079015000	0.934788000
7	-1.666769000	1.388202000	-0.931173000
6	-0.410913000	1.337071000	-0.530532000
7	-0.815601000	-0.131195000	1.334349000
6	0.046378000	0.587173000	0.594779000
34	-3.519654000	-0.988644000	1.766290000
6	-4.650798000	-0.217737000	0.423642000
6	-3.939324000	0.567151000	-0.432570000
34	1.038907000	2.238884000	-1.367790000
6	2.172709000	1.456164000	-0.029338000
6	1.457972000	0.682354000	0.833341000
1	-4.391056000	1.098803000	-1.262471000
1	1.904688000	0.159737000	1.669861000
14	-6.524828000	-0.463458000	0.409575000
14	3.998256000	1.906338000	0.057515000

6	-6.913136000	-1.873270000	1.630308000
6	-7.057211000	-0.808357000	-1.391585000
6	-7.204427000	1.221146000	0.993698000
6	5.006834000	0.483783000	0.837331000
6	4.615185000	2.250088000	-1.712451000
6	4.112525000	3.519147000	1.078497000
6	-8.697786000	1.471132000	0.728094000
1	-8.939651000	1.403371000	-0.335249000
1	-8.981720000	2.474656000	1.064504000
1	-9.334573000	0.759748000	1.260720000
6	-6.086675000	-1.714314000	-2.170541000
1	-6.410393000	-1.811719000	-3.212771000
1	-6.053990000	-2.720677000	-1.744764000
1	-5.067558000	-1.325044000	-2.169585000
6	-8.492641000	-1.357802000	-1.500427000
1	-7.044136000	0.181086000	-1.871463000
1	-8.555593000	-2.370953000	-1.094072000
1	-8.802147000	-1.411845000	-2.549828000
1	-9.224494000	-0.743792000	-0.972022000
6	-8.383531000	-1.939040000	2.079725000
1	-8.713256000	-1.009130000	2.547151000
1	-8.522161000	-2.741992000	2.812062000
1	-9.053764000	-2.145550000	1.241547000
6	-6.442156000	-3.248085000	1.121067000
1	-6.318793000	-1.629343000	2.522708000
1	-7.046584000	-3.581431000	0.273080000
1	-6.541167000	-4.004191000	1.907508000
1	-5.397511000	-3.239428000	0.801103000
6	-6.842998000	1.489358000	2.465023000
1	-5.771372000	1.375010000	2.647872000
1	-7.369840000	0.806168000	3.138205000

1	-7.122581000	2.508508000	2.753370000
1	-6.640277000	1.941137000	0.384411000
6	3.734098000	4.760828000	0.250637000
1	4.376203000	4.898635000	-0.621697000
1	3.810924000	5.665985000	0.862917000
1	2.699941000	4.697109000	-0.102515000
6	3.253459000	3.475443000	2.355108000
1	3.395317000	4.388886000	2.942980000
1	3.493105000	2.627962000	2.999024000
1	2.191821000	3.405831000	2.103338000
1	5.166148000	3.615138000	1.375915000
6	6.068369000	2.758671000	-1.712887000
1	6.757424000	1.979161000	-1.372404000
1	6.209170000	3.628366000	-1.065899000
1	6.379912000	3.044703000	-2.723232000
6	4.461869000	1.069045000	-2.685580000
1	3.978936000	3.065961000	-2.082089000
1	5.152001000	0.259093000	-2.433772000
1	4.693980000	1.382391000	-3.709362000
1	3.448912000	0.659799000	-2.685480000
6	4.584027000	-0.911037000	0.339354000
1	3.594779000	-1.183070000	0.714361000
1	5.290121000	-1.671016000	0.691733000
1	4.543586000	-0.974380000	-0.749007000
6	5.081726000	0.499024000	2.373500000
1	6.025002000	0.669295000	0.466262000
1	4.100197000	0.331674000	2.827083000
1	5.469893000	1.444101000	2.759741000
1	5.741351000	-0.299912000	2.729940000

3b

Xyz

0 1

6	-2.514618000	0.536758000	-0.276770000
6	-2.084516000	-0.081475000	0.936089000
7	-1.635516000	1.181144000	-1.060337000
6	-0.392641000	1.186891000	-0.620675000
7	-0.841664000	-0.075632000	1.375811000
6	0.037472000	0.568586000	0.592147000
34	-3.544093000	-0.915440000	1.833480000
6	-4.607480000	-0.294731000	0.389210000
6	-3.919307000	0.397676000	-0.546631000
34	1.066957000	2.020607000	-1.518213000
6	2.130096000	1.401187000	-0.073196000
6	1.442073000	0.708110000	0.862257000
1	-4.368773000	0.821933000	-1.434856000
1	1.891601000	0.283699000	1.750376000
1	-5.664939000	-0.512769000	0.380160000
1	3.187418000	1.619875000	-0.063832000

3c

Xyz

0 1

6	-2.556538000	0.720390000	-0.160870000
6	-2.118683000	0.105692000	1.048507000
7	-1.681160000	1.365899000	-0.949075000
6	-0.436850000	1.374238000	-0.514482000
7	-0.874374000	0.114035000	1.483110000
6	0.001001000	0.759545000	0.694903000
34	-3.576624000	-0.728701000	1.949036000
6	-4.668570000	-0.111476000	0.500090000
6	-3.961320000	0.578972000	-0.425539000
34	1.021099000	2.208614000	-1.415014000
6	2.112986000	1.591703000	0.034147000
6	1.405721000	0.901239000	0.959746000
1	-4.411225000	1.003994000	-1.314483000
1	1.855568000	0.476441000	1.848827000
6	-6.131313000	-0.413398000	0.487866000
6	3.575798000	1.893279000	0.046143000
1	-6.633008000	0.005223000	1.365709000
1	-6.315833000	-1.492112000	0.489064000
1	-6.594821000	0.011072000	-0.405348000
1	3.761397000	2.971748000	0.043588000
1	4.076790000	1.473060000	-0.831408000
1	4.039285000	1.468982000	0.939453000

3d

Xyz

0 1

6	-2.536511000	0.507921000	-0.201197000
6	-2.111163000	0.422179000	1.156897000
7	-1.638023000	0.687068000	-1.183664000
6	-0.383840000	0.771151000	-0.786780000
7	-0.856978000	0.506217000	1.553778000
6	0.041520000	0.685392000	0.571315000
34	-3.599885000	0.167139000	2.318425000
6	-4.687186000	0.214064000	0.738471000
6	-3.955333000	0.389039000	-0.388053000
34	1.104900000	1.026154000	-1.948285000
6	2.192159000	0.979213000	-0.368403000
6	1.460339000	0.804278000	0.758163000
1	-4.398631000	0.442444000	-1.374973000
1	1.903670000	0.750851000	1.745065000
6	-6.169410000	0.044472000	0.841234000
6	3.674300000	1.149519000	-0.471112000
6	-6.600276000	-1.343150000	1.347069000
1	-6.598972000	0.220760000	-0.150718000
1	-6.586018000	0.812545000	1.504186000
6	4.104262000	2.539100000	-0.972079000
1	4.090949000	0.384151000	-1.136962000
1	4.104387000	0.969830000	0.520105000
1	-6.162613000	-2.109213000	0.697428000
6	-8.120738000	-1.507910000	1.396802000
1	-6.181492000	-1.513452000	2.345613000
1	-8.535118000	-1.339758000	0.395503000
1	-8.547515000	-0.728142000	2.039161000
6	-8.550887000	-2.885280000	1.905599000

1	-8.161992000	-3.680963000	1.262786000
1	-9.639707000	-2.979240000	1.931242000
1	-8.176207000	-3.065275000	2.917966000
1	3.684968000	2.712761000	-1.969762000
6	5.624621000	2.704851000	-1.021666000
1	3.666425000	3.302521000	-0.319509000
1	6.051811000	1.926801000	-1.665954000
1	6.039265000	2.534558000	-0.020711000
6	6.053900000	4.083678000	-1.527268000
1	5.679889000	4.265402000	-2.539612000
1	7.142650000	4.178720000	-1.551772000
1	5.663689000	4.877702000	-0.883121000

3e

Xyz

0 1

6	-2.489438000	0.692587000	-0.370935000
6	-2.046056000	-0.022797000	0.782086000
7	-1.614935000	1.396261000	-1.111930000
6	-0.368817000	1.362618000	-0.686538000
7	-0.799938000	-0.056440000	1.207478000
6	0.074567000	0.647229000	0.466480000
34	-3.498203000	-0.917580000	1.626002000
6	-4.600141000	-0.190047000	0.232042000
6	-3.889546000	0.577058000	-0.640328000
34	1.083335000	2.257379000	-1.530470000
6	2.185283000	1.529800000	-0.136547000
6	1.474683000	0.762718000	0.735842000
1	-4.331561000	1.052362000	-1.506133000
1	1.916707000	0.287380000	1.601623000
6	-6.036025000	-0.469741000	0.203439000
6	3.621188000	1.809405000	-0.108033000
6	4.509743000	0.882826000	0.462257000
6	4.145927000	2.996734000	-0.640341000
6	5.511101000	3.254330000	-0.595158000
6	5.873037000	1.145023000	0.509862000
6	6.380365000	2.331666000	-0.017539000
1	4.127236000	-0.055001000	0.846327000
1	6.543790000	0.415716000	0.949710000
1	5.895844000	4.180320000	-1.006946000
1	7.444863000	2.532183000	0.016205000
1	3.475883000	3.732548000	-1.070330000
6	-6.924533000	0.456556000	-0.367385000
6	-6.560674000	-1.657342000	0.735232000

6	-8.287901000	0.194632000	-0.414378000
6	-8.795367000	-0.991385000	0.114292000
6	-7.925920000	-1.914663000	0.690655000
1	-5.890521000	-2.393562000	1.164356000
1	-8.310590000	-2.840880000	1.102001000
1	-8.958605000	0.923694000	-0.854707000
1	-9.859771000	-1.192280000	0.079840000
1	-6.541918000	1.393957000	-0.752373000

3f

Xyz

0 1

6	-3.568478000	0.758727000	-0.163496000
6	-3.137995000	-0.128997000	0.867996000
7	-2.678230000	1.536939000	-0.805064000
6	-1.428695000	1.395735000	-0.413360000
7	-1.889236000	-0.266190000	1.263593000
6	-0.997255000	0.503274000	0.613845000
34	-4.611052000	-1.093633000	1.590834000
6	-5.705905000	-0.119645000	0.348431000
6	-4.975762000	0.737884000	-0.417638000
34	0.046044000	2.351307000	-1.144973000
6	1.139111000	1.384922000	0.104418000
6	0.409723000	0.526205000	0.869744000
1	-5.416744000	1.391561000	-1.158705000
1	0.844629000	-0.087393000	1.647790000
6	-7.146764000	-0.358716000	0.290460000
6	2.584386000	1.600082000	0.140117000
6	3.446475000	0.574940000	0.552077000
6	3.157169000	2.827448000	-0.230506000
6	4.529334000	3.015270000	-0.179824000
6	4.821991000	0.772235000	0.603366000
6	5.392676000	1.994516000	0.238846000
1	3.036868000	-0.393979000	0.811320000
1	5.453293000	-0.047637000	0.921478000
1	4.944431000	3.976496000	-0.466323000
1	2.516929000	3.646902000	-0.538022000
6	-7.856537000	-0.135636000	-0.900675000
6	-7.864279000	-0.809515000	1.408201000
6	-9.226625000	-0.346252000	-0.961281000

6	-9.942835000	-0.792742000	0.154478000
6	-9.234765000	-1.021290000	1.337869000
1	-7.347224000	-0.970076000	2.347766000
1	-9.768333000	-1.363326000	2.218777000
1	-9.752066000	-0.169526000	-1.894331000
1	-7.323316000	0.184596000	-1.787635000
6	-11.419917000	-1.079086000	0.066301000
6	-11.703922000	-2.528896000	-0.371021000
1	-11.887966000	-0.394421000	-0.649571000
1	-11.884034000	-0.886632000	1.037616000
6	-13.195107000	-2.854644000	-0.516689000
1	-11.244016000	-3.214721000	0.350344000
1	-11.198240000	-2.707134000	-1.326030000
6	-13.983588000	-2.821115000	0.797369000
1	-13.295856000	-3.851561000	-0.961963000
1	-13.652073000	-2.155705000	-1.229595000
6	-15.453515000	-3.205860000	0.615471000
1	-13.927273000	-1.821356000	1.241347000
1	-13.510910000	-3.503088000	1.515182000
1	-15.955433000	-2.522989000	-0.077592000
1	-15.996486000	-3.175501000	1.563982000
1	-15.548152000	-4.217632000	0.208791000
6	6.884821000	2.254667000	0.271822000
6	7.771182000	1.094139000	0.724042000
1	7.069194000	3.117885000	0.923989000
1	7.200886000	2.573643000	-0.729486000
6	9.258481000	1.455268000	0.720103000
1	7.609725000	0.229371000	0.069578000
1	7.480515000	0.778090000	1.732918000
6	10.162711000	0.303610000	1.167225000
1	9.424654000	2.320691000	1.374481000

1	9.552335000	1.775147000	-0.287922000
6	11.648087000	0.670727000	1.159192000
1	9.994335000	-0.560438000	0.513197000
1	9.868329000	-0.014702000	2.174547000
1	11.975971000	0.961955000	0.156334000
1	12.270027000	-0.168384000	1.482236000
1	11.849096000	1.512209000	1.829679000

3g

Xyz

0 1

6	-3.551303000	0.449000000	-0.152569000
6	-3.065009000	-0.472721000	0.823545000
7	-2.702582000	1.262840000	-0.803833000
6	-1.436104000	1.127580000	-0.471448000
7	-1.799223000	-0.601785000	1.162160000
6	-0.949886000	0.208481000	0.506993000
34	-4.487011000	-1.492845000	1.566949000
6	-5.645521000	-0.487468000	0.414431000
6	-4.967153000	0.415962000	-0.346729000
34	-0.011677000	2.128210000	-1.235991000
6	1.145621000	1.139108000	-0.067579000
6	0.465527000	0.245797000	0.704399000
1	-5.445706000	1.093346000	-1.041501000
1	0.935981000	-0.390485000	1.442210000
6	-7.088227000	-0.732349000	0.413705000
6	2.589614000	1.375690000	-0.080628000
6	3.471548000	0.419006000	0.444256000
6	3.132128000	2.551282000	-0.615546000
6	4.506478000	2.760534000	-0.625110000
6	4.842056000	0.644060000	0.444235000
6	5.374651000	1.813246000	-0.093063000
1	3.089696000	-0.514768000	0.834231000
1	2.481066000	3.321779000	-1.009439000
6	-7.872064000	-0.349879000	-0.685242000
6	-7.725126000	-1.346286000	1.499977000
6	-9.245143000	-0.559522000	-0.681876000
6	-9.871847000	-1.170579000	0.400980000
6	-9.097947000	-1.564744000	1.487211000

1	-7.154539000	-1.635214000	2.373613000
1	-7.406934000	0.095744000	-1.553948000
1	-10.939464000	-1.339035000	0.395825000
1	6.442284000	1.979829000	-0.099607000
6	-9.741736000	-2.286089000	2.641167000
6	-10.067865000	-0.077009000	-1.847521000
6	5.053975000	4.003567000	-1.275087000
6	5.750620000	-0.377162000	1.076570000
9	-11.214713000	-0.772865000	-1.978710000
9	-10.407926000	1.223387000	-1.702564000
9	-9.393931000	-0.178566000	-3.012255000
9	-11.034694000	-1.937939000	2.794833000
9	-9.710953000	-3.625272000	2.459796000
9	-9.109361000	-2.032666000	3.805888000
9	5.789640000	-0.231244000	2.419821000
9	5.333265000	-1.637690000	0.832453000
9	7.017349000	-0.274649000	0.629045000
9	4.258438000	5.072522000	-1.059082000
9	5.151054000	3.851889000	-2.614699000
9	6.284462000	4.312864000	-0.821236000

6.4 Visualization of the HOMO and LUMO Orbitals

Table S7. Visualization of the HOMO and LUMO Orbitals of **3a-g**.

Compound	**3a**	**3b**	**3c**
HOMO	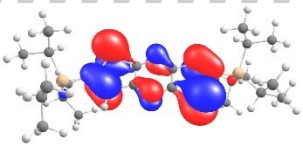	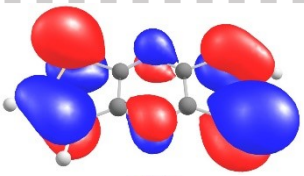	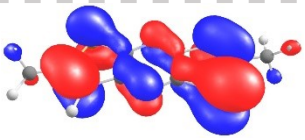
LUMO	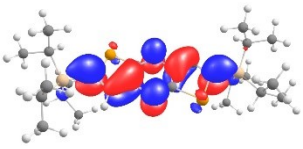	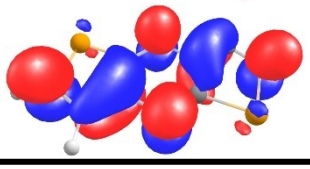	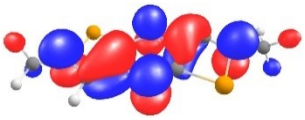
Compound	**3d**	**3e**	**3f**
HOMO	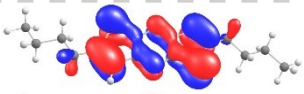	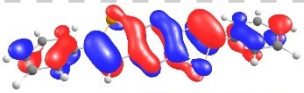	
LUMO		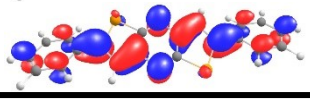	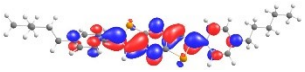
Compound	**3g**		
HOMO	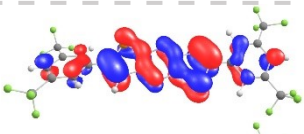		
LUMO	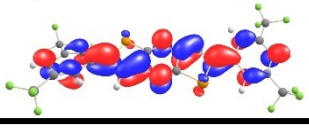		

6.5 Investigation of Short-Contact Interactions by DFT calculation

A bond decomposition analysis[11] was performed with ADF.[12] This calculation was also performed on a BLYP-D3[13]/TZ2P[14]/ZORA[15-17] level of theory in the gas phase to determine the total bonding energy.

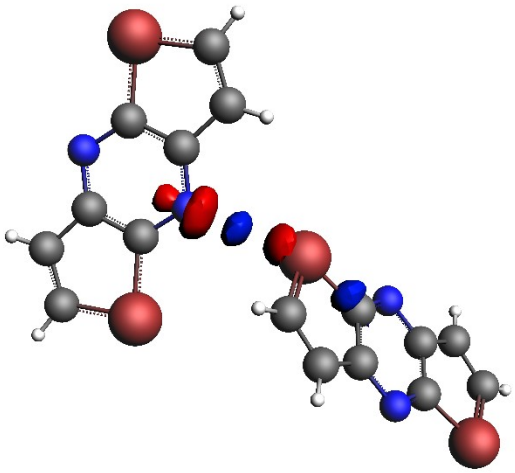

Figure S40. Visualization of the intermolecular non-bonding interacting orbitals of selenium and nitrogen in the single crystal structure of **3b**.

Table S8. Computed Energies of **3b**.

E_{Pauli} [kcal/mol]	E_{el} [kcal/mol]	E_{disp} [kcal/mol]	E_{Orb} [kcal/mol]	E_{tot} [kcal/mol]
11.87	-7.61	-6.72	-3.55	-6.01

7 References

(1) G. R. Fulmer, A. J. M. Miller, N. H. Sherden, H. E. Gottlieb, A. Nudelman, B. M. Stoltz, J. E. Bercaw and K. I. Goldberg, NMR Chemical Shifts of Trace Impurities: Common Laboratory Solvents, Organics and Gases in Deuterated Solvents Relevant to the Organometallic Chemist, *Organometallics*, 2010, **29**, 2176-2179.

(2) P. Meti, E.-S. Lee, J.-W. Yang and Y.-D. Gong, Regioselective synthesis of dipyrrolopyrazine (DPP) derivatives *via* metal free and metal catalyzed amination and investigation of their optical and thermal properties, *RSC Adv.* 2017, **7**, 18120-18131.

(3) R. Heckershoff, T. Schnitzer, T. Diederich, L. Eberle, P. Krämer, F. Rominger, M. Rudolph and A. S. K. Hashmi, Efficient Synthesis of Dipyrrolobenzenes and Dipyrrolopyrazines via Bidirectional Gold Catalysis: a Combined Synthetic and Photophysical Study, *J. Am. Chem. Soc.* 2022, **144**, 8306-8316.

(4) C. Hüßler, J. Kahle, M. C. Dietl, P. Krämer, F. Rominger, M. Rudolph and A. S. K. Hashmi, Facile two-step synthesis of *para*-dithienopyrazines, *Org. Chem. Front.*, 2023, **10**, 3726–3731.

(5) F. Neese, Software update: The ORCA program system – Version 5.0, *WIREs Comput. Mol. Sci.* 2022, **12**, e1606.

(6) A. D. Becke, Density-functional thermochemistry. III. The role of exact exchange, *The Journal of Chemical Physics*, 1993, **98**, 5648–5652.

(7) C. Lee, W. Yang and R. G. Parr, Development of the Colle-Salvetti correlation-energy formula into a functional of the electron density, *Phys Rev B Condens Matter*, 1988, **37**, 785–789.

(8) S. H. Vosko, L. Wilk and M. Nusair, Accurate spin-dependent electron liquid correlation energies for local spin density calculations: a critical analysis, *Can. J. Phys.*, 1980, **58**, 1200–1211.

(9) P. J. Stephens, F. J. Devlin, C. F. Chabalowski and M. J. Frisch, Ab Initio Calculation of Vibrational Absorption and Circular Dichroism Spectra Using Density Functional Force Fields, *J. Phys. Chem.*, 1994, **98**, 11623–11627.

(10) L. A. Curtiss, J.-P. Blandeau, N. E. Davis, R. C. Binning and L. Radom, Extension of Gaussian-2 theory to molecules containing third-row atoms Ga-Kr, *J. Chem. Phys.*, 1995, **103**, 6104-6113.

(11) M. P. Mitoraj, A. Michalak and T. Ziegler, A Combined Charge and Energy Decomposition Scheme for Bond Analysis, *J. Chem. Theory. Comput.*, 2009, **5**, 962–975.

(12) G. te Velde, F. M. Bickelhaupt, E. J. Baerends, C. Fonseca Guerra, S. J. A. van Gisbergen, J. G. Snijders and T. Ziegler, Chemistry with ADF, *J. Comput. Chem.*, 2001, **22**, 931–967.

(13) S. Grimme, A. Hansen, J. G. Brandenburg and C. Bannwarth, Dispersion-Corrected Mean-Field Electronic Structure Methods, *Chem. Rev.*, 2016, **116**, 5105–5154.

(14) E. van Lenthe and E. J. Baerends, Optimized Slater-type basis sets for the elements 1-118, *J. Comput. Chem.*, 2003, **24**, 1142–1156.

(15) E. van Lenthe, E. J. Baerends and J. G. Snijders, Relativistic regular two-component Hamiltonians, *J. Chem. Phys.*, 1993, **99**, 4597–4610.

(16) E. van Lenthe, E. J. Baerends and J. G. Snijders, Relativistic total energy using regular approximations, *J. Chem. Phys.*, 1994, **101**, 9783–9792.

(17) E. van Lenthe, A. Ehlers and E.-J. Baerends, Geometry optimizations in the zero order regular approximation for relativistic effects, *J. Chem. Phys.*, 1999, **110**, 8943–8953.